UNLV University Libraries
University of Nevada, Las Vegas

UNLV Theses, Dissertations, Professional Papers, and Capstones

12-1-2013

Assessing Different Zeolitic Adsorbents for their Potential Use in Kr and Xe Separation

Breetha Alagappan
University of Nevada, Las Vegas, alagappa@unlv.nevada.edu

Follow this and additional works at: https://digitalscholarship.unlv.edu/thesesdissertations

Part of the Inorganic Chemistry Commons, Nanoscience and Nanotechnology Commons, and the Nuclear Engineering Commons

Repository Citation

Alagappan, Breetha, "Assessing Different Zeolitic Adsorbents for their Potential Use in Kr and Xe Separation" (2013). *UNLV Theses, Dissertations, Professional Papers, and Capstones*. 1967.
https://digitalscholarship.unlv.edu/thesesdissertations/1967

This Thesis is protected by copyright and/or related rights. It has been brought to you by Digital Scholarship@UNLV with permission from the rights-holder(s). You are free to use this Thesis in any way that is permitted by the copyright and related rights legislation that applies to your use. For other uses you need to obtain permission from the rights-holder(s) directly, unless additional rights are indicated by a Creative Commons license in the record and/or on the work itself.

This Thesis has been accepted for inclusion in UNLV Theses, Dissertations, Professional Papers, and Capstones by an authorized administrator of Digital Scholarship@UNLV. For more information, please contact digitalscholarship@unlv.edu.

ASSESSING DIFFERENT ZEOLITIC ADSORBENTS FOR THEIR POTENTIAL USE IN Kr AND Xe SEPARATION

by

Breetha Alagappan

Bachelor of Science in Chemistry
Manonmaniam Sundaranar University, India
2002

A thesis submitted in partial fulfillment
of the requirements for the

Master of Science – Chemistry

Department of Chemistry
College of Sciences
The Graduate College

University of Nevada, Las Vegas
December 2013

THE GRADUATE COLLEGE

We recommend the thesis prepared under our supervision by

Breetha Alagappan

entitled

Assessing Different Zeolitic Adsorbents for their Potential Use in Kr and Xe Separation

is approved in partial fulfillment of the requirements for the degree of

Master of Science - Chemistry

Department of Chemistry

Paul Forster, Ph.D., Committee Chair

Balakrishnan Naduvalath, Ph.D., Committee Member

Clemens Heske, Ph.D., Committee Member

Venkatesan Muthukumar, Ph.D., Graduate College Representative

Kathryn Hausbeck Korgan, Ph.D., Interim Dean of the Graduate College

December 2013

ABSTRACT

Assessing Different Zeolitic Adsorbents for their Potential Use in Kr and Xe Separation

by

Breetha Alagappan

Dr. Paul Forster, Examination Committee Chair

Assistant Professor of Chemistry

University of Nevada, Las Vegas

Separation of Kr from Xe is an important problem in spent nuclear fuel fission gas management. The energy intensive and expensive cryogenic distillation method is currently used to separate these gases. In this thesis, we have carried out the research into appropriate sorbents for the separation of Kr and Xe using pressure swing adsorption. We have examined zeolites using gas adsorption studies as they have the potential to be more cost effective than other sorbents. Zeolites are microporous aluminosilicates and have ordered pore structures. The pores in zeolites have extra-framework cations are substantially free to move. The mobility of cations and the uniformity in pore size permits the separation and removal of gases in zeolites. In our experiment, first, we have measured adsorption isotherms with same zeolitic framework but with different cations. Second, we have measured the adsorption isotherm with different zeolitic frameworks but

with same cation. Using these adsorption isotherms, we have calculated the initial heats of adsorption to find out the strength of interaction between the zeolitic framework and the gases. Finally, we have compared the difference in the initial heats of adsorption to find the suitable zeolite that has the highest selectivity of Xe over Kr. In conclusion, we have found out that K LSX seems to have higher potential among the zeolites that we have compared for the separation of Kr from Xe with the differential heats of adsorption for Xe vs Kr as ~ 7.4 kJ/mol.

ACKNOWLEDGEMENTS

I would like to express my sincere gratitude to everyone that contributed to the success of this thesis. I would like to thank the opportunity that Prof. Paul Forster provided me to work in this NEUP project. His support and guidance has shaped me in many ways both professionally and personally. Thank you for everything you have done for me. Financial support provided throughout the course of the study is gratefully acknowledged. I am thankful for the dedication of Prof. Heske, Prof. Naduvalath and Prof. Muthukumar as committee members for my thesis.

I wish to acknowledge my deep sense of gratitude to Dr. Keith Lawler, for his critical suggestions and untiring help during the course of this investigation. I am thankful to Julie Bertoia, Grace, Jason, Eric Knight, Zeric Hulvey for their time and help in my research. The help rendered by Mrs.Katey Forster is thankfully acknowledged. I am grateful to all my friends and family members for their support throughout my research. I would not have completed this journey without the patient and constant encouragement and support from my husband Arun Asokan. I dedicate this thesis to my beloved husband.

TABLE OF CONTENTS

ABSTRACT iii

ACKNOWLEDGEMENTS v

TABLE OF CONTENTS vi

LIST OF TABLES viii

LIST OF FIGURES ix

CHAPTER 1 INTRODUCTION 1
1.1. Motivation and scope 1
1.2. Zeolites 2
1.2.1. Formation of zeolites 2
1.2.2. Structure and properties of zeolites 3
1.2.3. Application of zeolites 6
1.2.3.1. Adsorption and separation 6
1.2.3.2. Catalysis 8
1.2.3.3 Ion Exchange 9
1.2.3.3.1 Cation exchange principle 10
1.2.4. Different framework types 12
1.2.4.1. LTA 12
1.2.4.2. GIS 14
1.2.4.3. RHO 15
1.2.4.4. FAU 16
1.3. Literature Survey in gas separation in FAU zeolitic framework 18
1.4. Adsorption and gas separation 19
1.4.1. Adsorption- Definition 19
1.4.2. Adsorbents and Adsorbates 20
1.4.3. Properties of Kr and Xe 20
1.4.4 Adsorption isotherms 21
1.4.5. Factors affecting adsorptive gas separation 23
1.4.5.1. Adsorbate and Adsorbent interactions 23
1.4.5.2. Surface structure of adsorbents 24
1.5. Heat of adsorption using Clausius – Clapeyron equation 25

CHAPTER 2 EXPERIMENTAL PROCEDURES 26
2.1. Material synthesis 26
2.1.1. LTA - Synthesis Procedure 26
2.1.2. RHO - Synthesis Procedure 27
2.1.3. GIS - Synthesis Procedure 27

2.1.4. FAU LSX - Synthesis Procedure.....28
2.2. Ion exchange 28
2.2.1. LTA Ca.....29
2.2.2. RHO Ca..... 29
2.2.3. GIS Ca.....30
2.2.4. FAU LSX Ca.....30
2.2.5. FAU LSX Li.....31
2.2.6. FAU LSX Na.....31
2.2.7. FAU LSX K.....32
2.2.8. FAU LSX Rb..... 32
2.2.9. FAU LSX Cs..... 33
2.3. Material characterization..... 33
2.3.1. X-ray powder diffraction..... 33
2.3.2. Elemental analysis..... 35
2.3.2.1 Experimental and apparatus..... 36
2.4. Adsorption isotherm measurement.....39

CHAPTER 3 RESULTS AND DISCUSSION..... 40
3.1. Adsorption isotherm measurement 41
3.2. Gas adsorption studies in Kr and Xe using FAU LSX but with different alkali cations 42
3.2.1. Heats of adsorption in FAU LSX zeolites with different alkali cations..... 44
3.3. Gas adsorption studies in Kr and Xe with same cation but with different zeolite framework..... 48
3.3.1. Extrapolated initial heats of adsorption in Ca ion-exchanged zeolitic frameworks..... 50
3.4. Discussion of results..... 52
3.5. Conclusion 58

APPENDIX I SUPPLEMENTARY INFORMATION FOR CHAPTER 2..... 59

APPENDIX II SUPPLEMENTARY INFORMATION FOR CHAPTER 3..... 60

REFERENCES 72

VITA.....81

LIST OF TABLES

Table 1.1 Physical Parameters of Kr and Xe.....21
Table 2.1 Unit cell composition, % ion exchange and Si/Al ratio determined from ICP- AES 37
Table 2.2 ICP AES instrumental specifications..... 38
Table 3.1 As- synthesized zeolites in Lab.....41
Table 3.2 Kr and Xe atoms per supercage at 700 mm Hg in FAU LSX.....43
Table 3.3 Extrapolated initial heats of adsorption values in Kr and Xe with different alkali metal ion-exchanged FAU LSX zeolite.....46
Table 3.4 Kr and Xe atoms per supercage at 700 mm Hg in Ca ion-exchanged FAU LSX and LTA 48
Table 3.5 Extrapolated initial heats of adsorption values with Kr and Xe in calcium metal ion-exchanged LTA, FAU LSX, GIS and RHO zeolite frameworks..... 51
Table 3.6 Polarizability and atomic number of cations and gases.....53

LIST OF FIGURES

Figure 1.1 Tetrahedron-primary building unit ……3
Figure 1.2 Development of zeolite structures……4
Figure 1.3 Secondary Building Units (SBU's) in zeolites. The corner of the polyhedral represents tetrahedral atoms……...5
Figure 1.4 Size-selective separation of gas molecules in zeolite ZSM-5 by trapping them inside the cages ……...7
Figure 1.5 Types of shape selectivity exhibited by zeolites……...8
Figure 1.6 Extra-framework Na metal ion is shown in purple color in Zeolite 4A…..10
Figure 1.7 Cation exchange isotherm (adapted)…….. 11
Figure 1.8 Pores in zeolite A (IZA code LTA) (a) the sodalite cage (b) the α-cavity (c) the three-dimensional channel system, and (d) the 8-ring defining the 4.1Å effective channel width……..13
Figure 1.9 Comparison of pore sizes of different framework structures……13
Figure 1.10 Structure of Gismondine Zeolite..... 14
Figure 1.11 GIS double crank shaft chain as a composite building unit..... 15
Figure 1.12 Double crank shaft chains in GIS zeolite..... 15
Figure 1.13 Zeolite RHO.....16
Figure 1.14 α cage in zeolite RHO.....16
Figure 1.15 The framework of faujasite zeolite 18
Figure 1.16 Classification of adsorption isotherms defined by IUPAC.....21
Figure 2.1 X-ray diffraction patterns of FAU LSX zeolites..... 34
Figure 3.1 Kr and Xe adsorption isotherms in the alkali metal ion-exchanged FAU LSX at different temperatures.....42
Figure 3.2 Heats of adsorption curves in Kr and Xe with different alkali metal ion-exchanged zeolite FAU LSX and extrapolations to zero coverage 45
Figure 3.3 Difference in the Heats of adsorption curves in Kr and Xe with different alkali metal ion-exchanged zeolite FAU LSX..... 46
Figure 3.4 Kr and Xe adsorption isotherms in the calcium ion-exchanged zeolites with different frameworks..... 49
Figure 3.5 Heats of adsorption curves in Kr and Xe with calcium ion exchanged Zeolite.....50
Figure 3.6 Heats of adsorption curves of Kr and Xe in calcium ion-exchanged with LTA and FAU LSX zeolitic frameworks.....51
Figure 3.7 Proportional term of the Polarization energy vs. HOA in Ar (Maurin), Kr and Xe with Li, Na and K cations.....55
Figure 3.8 Ar, Kr and Xe dispersion interaction with the alkali cations in the zeolite framework vs HOA 56

CHAPTER 1

INTRODUCTION

The motivation behind this thesis is to find a suitable zeolitic sorbent to separate Kr from Xe during nuclear reprocessing technology. Our aim is to identify a zeolitic material that is affordable and can be used to practically separate Kr from Xe through pressure swing adsorption. In this project, we have carried out the research into the separation of these gases by using zeolites in gas adsorption studies.

Section 1.1 provides information on motivation and scope of this research. Sections 1.2.1, 1.2.2 and 1.2.3 give details about zeolites, their formation, structure and properties. The applications of zeolites in adsorption, separation and catalysis and ion exchange are discussed in section 1.2.3. A brief description of cation exchange and its principle is outlined in section 1.2.3.3.1. In section 1.2.4, different zeolitic frameworks that are chosen for this study are discussed in detail. Literature survey in gas adsorption and separation in FAU zeolite framework is outlined in section 1.3. Finally this chapter concludes with a detailed discussion on adsorption and gas separation in sections 1.4 and 1.5.

1.1 Motivation and scope

The noble gases Kr and Xe, in spite of their low reactivity, have importance in research and industry owing to their applications in various fields. Xenon is used as general anesthetics in medical imaging, radiation detection, photographic flashes, propellant in modern ion thrusters for spacecraft, etc. Krypton finds its use in electric lamp bulbs, electronic devices, in high powered electric arc lights used in airports and so on.

However, the only source for these gases is atmosphere, which contains 1 ppm of Kr and 0.08 ppm of Xe. Both Kr and Xe are obtained as a byproduct of fractional distillation of air at cryogenic temperature. Additionally, with current reprocessing technology, the noble gasses Kr and Xe come off from spent fuel as a mixture. The conventional method to separate these gases from spent fuel is the cryogenic distillation process which is energy intensive and expensive.[1] Even after cryogenic distillation, trace amounts of radioactive Kr^{85} are present in the Xe phase beyond its permissible level.[2] Consequently, there is a need to separate these gases from one another during nuclear reprocessing cost-effectively. In this project, we will carry out the research assessing different zeolitic adsorbents for their potential use in Kr and Xe separation using gas adsorption studies.

1.2. Zeolites

When we heat a glass of water, we can see steam rise off sooner or later as it comes to boil. We certainly don't expect the same thing to happen when we heat a rock, unless it's a special kind of rock called “zeolite” which “traps water” inside of it. In 1756, Swedish geologist Axel Cronstedt (1722–1765) coined the name "zeolite" which literally means "boiling stone".[3] Today, the term refers to over 250 unique minerals that have all kinds of interesting uses, from water softeners to animal food and industrial catalysts.

1.2.1 Formation of zeolites

In nature, zeolites are typically formed when volcanic ash chemically reacts with saline water at a temperature range of 27°C to 55°C with a pH range approximately between 9 and 10. Such reactions complete in 50 – 50,000 years.[4] During this process, they are often contaminated with species like Fe^{2+}, quartz, SO_4^{2-} and other zeolites. This rarely results in

phase pure zeolite. At the same time, synthetic zeolites have advantages over the natural zeolite, as they can be synthesized with phase purity and uniformity. Moreover, synthetic zeolites can be tailored to a wide range of pore sizes not present in natural zeolites. The raw materials needed to synthesize zeolites are primarily the earth-abundant silica and alumina.

1.2.2 Structure and properties of zeolites

According to IUPAC[5] microporous materials have pore size between 2 – 20 Å, mesoporous materials have pore size between 20 – 500 Å and macroporous materials have pore size greater than 500 – 1000 Å. The microporous and mesoporous materials together are called nanoporous materials. Activated carbon, silca gel, metal organic framework materials and zeolites are typical examples of nanoporous materials.

Figure 1.1. Tetrahedron-primary building unit[6]

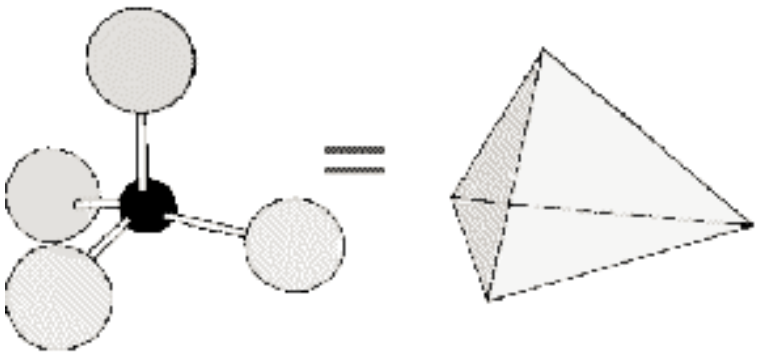

Zeolites are microporous crystalline aluminosilicates. They have a three dimensional framework of TO_4 tetrahedra (T= Al, Si) that forms the primary building units (Figure 1.1). These tetrahedra are linked to form secondary building units (Figure 1.3) of polyhedra such as cubes, octahedra etc. The Al and Si atoms are present at the corners of

tetrahedral units which are linked by a common oxygen atom. These corner-sharing tetrahedra are linked to form intracrystalline cavities and cages called pores which form the tertiary building units. The 1°, 2°and 3° building units together form the framework in zeolite structures (Figure 1.2).

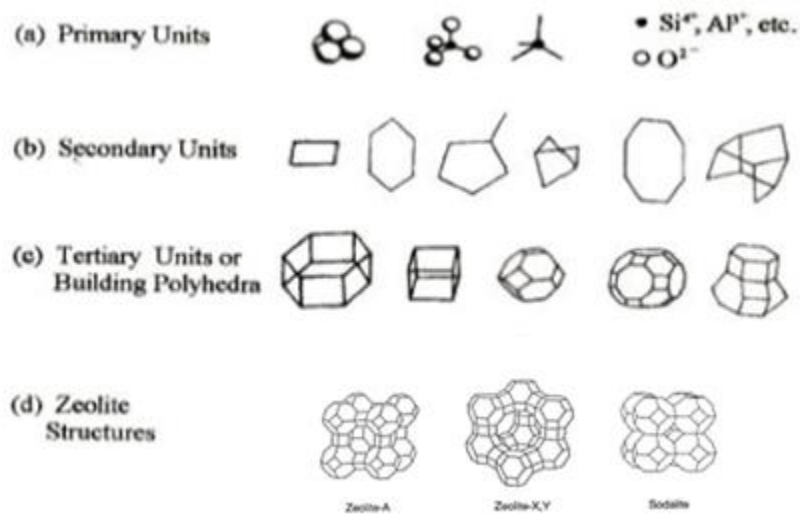

Figure 1.2. Development of zeolite structures[7]

The crystal chemistry of zeolites can be understood as follows. A silicon atom coordinates with four oxygen atoms in a tetrahedral geometry. A SiO_4 unit has -4 charge, where Si atom is in formally +4 oxidation state and the oxygen atom is in formally -2 oxidation state. But the SiO_4 unit is neutral in the zeolite framework, as oxygen atom bridges the SiO_4 units and makes the neutral SiO_2 framework.

However when an Al atom with a +3 valency substitutes a Si atom, a negative charge is introduced in the framework. To compensate, a positively charged cation from alkali metals (M+), e.g., Na^+, K^+ and alkaline earth metals (M^{2+}), e.g., Ca^{2+}, Ba^{2+}, or organic amines (especially quaternary amines) present in the synthesis are held in the interstices of the zeolite structure on crystallization. Thus, the charge balance is maintained in

zeolites. According to Lowenstein's rule,[8] adjacent AlO_4^- tetrahedra cannot be neighbors in the framework as the Al-O-Al linkages are forbidden. The lower limit of Si/Al ratio has to be one.

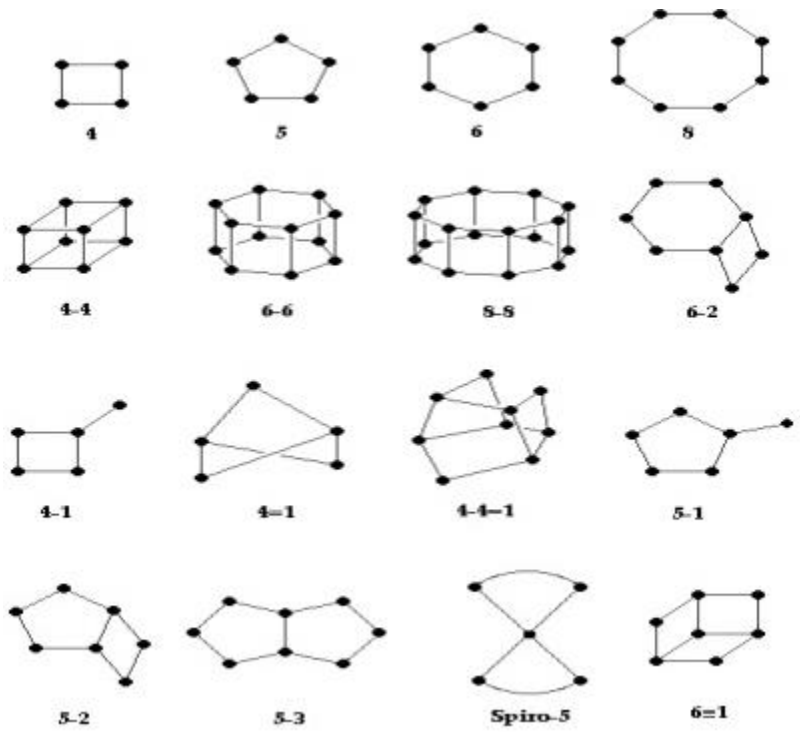

Figure 1.3. Secondary Building Units (SBU's) in zeolites.[9] The corner of the polyhedra represents tetrahedral atoms.

Zeolites have the chemical composition: $Mx/n[(AlO_2)x(SiO_2)y]\cdot ZH_2O$ where x and y are integers, y/x equal to or greater than 1, n is the valency of cation M and Z is the number of water molecules in each unit cell. The Si/Al ratio varies between 1to∞ where a completely siliceous zeolite (Si/Al = ∞) would be a polymorph of SiO_2. Pure silica zeolites are hydrophobic in nature whereas high alumina content in the zeolite framework makes them more attracted to polar molecules like water as they have more charge - balancing cations. The framework of zeolite varies with synthesis conditions. Different

zeolite-like molecular sieves such as aluminophosphates,[10, 11] gallophosphates,[12] and silicoaluminophosphates[5] can be synthesized by either total or partial replacement of Si and Al atoms in the framework.

Zeolites are also called molecular sieves as they can be used to separate molecules based on their sizes. More than 190 zeolites have been recognized and 48 naturally-occurring zeolites are identified.[13] The IZA Structure Commission assigns a three letter code derived from the name of the zeolite or "type material", e.g., LTA for Linde-type zeolites A, FAU for zeolites with a faujasite topology, e.g., zeolites LSX, X and Y, MFI for the ZSM-5 and silicate topologies. Some examples of the naturally occurring zeolites are faujasite, clinoptilolite, heulandite, natrolite and chabazite. Type A, X, Y and ZSM 5 zeolites are the common zeolites used commercially for ion exchange, adsorption and separation (Figure 1.4) and catalytic properties.[14]

1.2.3 Application of zeolites

The ordered pore structures, high surface areas, high resistance to temperature and also economical cost have made zeolites important commercially.

1.2.3.1 Adsorption and separation

The ability of zeolites to adsorb and exclude molecules based on their shape and size form the basis for adsorption and separation of molecules. Adsorption and separation is further discussed in detail in sections 1.4 and 1.5. Molecules with bigger kinetic diameter than the pore size of the zeolites are “sieved.” This sieving property of zeolites has earned them the name “molecular sieves.”[15] For example, the zeolite ZSM-5 finds its use[16] commercially in the isomerization of meta-xylene to para-xylene (Figure 1.5B) and in the

conversion of methanol to gasoline, thus acting as a shape-selective catalyst. Molecules can also be distinguished based on their electrostatic interactions with the cations. Thus zeolites containing cations are used as desiccants and in gas separation.[17, 18]

Potassium-exchanged zeolite 3A[1] is used in the dehydration of gases as it can adsorb only water and ammonia and excludes other gases like O_2, N_2 and hydrocarbons. In another example, calcium-exchanged zeolite 5A selectively separates[19] the linear paraffin from the hydrocarbon streams (Figure 1.5A). Zeolites A, X, and Y have dominated commercially in gas separation and purification since their invention. Li LSX[20] is at present the best commercial adsorbent for air separation. The Parex process of Universal Oil Products[21, 22]and the Eluxyl[23] developed at IFP uses faujasite zeolite Y to separate p-xylene from the mixture of isomers of xylene and ethyl benzene.

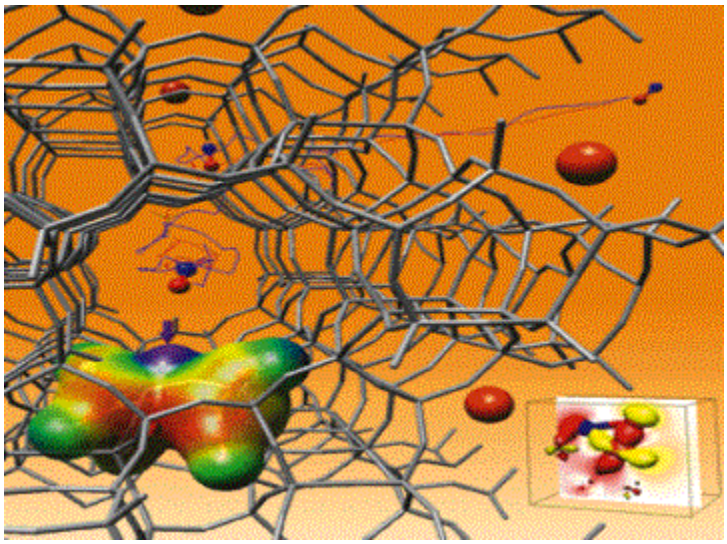

Figure 1.4. Size-selective separation of gas molecules in zeolite ZSM-5 by trapping them inside the cages[24]

1.2.3.2 Catalysis

Unlike other catalyst systems, where the catalytic activity is restricted to external surfaces, in zeolites more than 98% of the total surface area is typically internal. This forms the basis of synthetic zeolites being used as a catalyst in petrochemical refineries.[25] An exceptional property of zeolite catalysts is that they can distinguish chemical compounds based on their specific molecular structure called molecular sieving. The geometry of the zeolitic pores can also exert a steric influence in a reaction, thus controlling the access to the reactants and products.

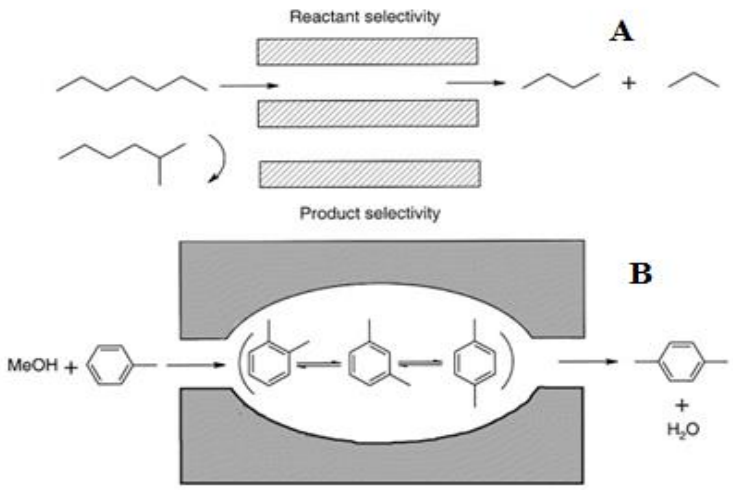

Figure1.5. Types of shape selectivity exhibited by zeolites[26]

As a result, zeolites are effective shape-selective catalysts. Unlike the other heterogeneous catalysts, zeolites show unusually high selectivity and thermal stability. Commercially, high selectivity is preferred over a high catalytic activity. The catalytic activity of zeolites largely finds its use in petroleum refinery: ZSM-5 with H^+ cation is

used in hydrocarbon conversion (Figure 1.5A).[27] It is also used in the isomerization of xylene (Figure 1.5B) from meta to para-xylene.[10]

1.2.3.3 Ion Exchange

The extra-framework cations in zeolites are loosely bound to the zeolitic framework. These ions can be ion exchanged with any other metal ion in an aqueous solution. This ion exchange property in zeolites has helped researchers to explore new avenues in catalytic applications. The sodium ions in Zeolite 4A (Figure 1.6), can be exchanged for $Ca^{2+}$and Mg^{2+} ions in hard water to soften it. It is used as builders in detergents to remove calcium and magnesium hardness, enhancing the washing efficiency.[28] Otherwise, these ions will react with detergents to form an insoluble mix called scum and reduce the surfactant efficiencies. This unique ion exchange property of zeolites has a great potential to be effectively used as sorbent materials for a large number of water treatment applications, such as water softening, ammonia removal from sewage, fertilizer factory wastewaters, etc. Heavy metals and radioactive isotopes from nuclear effluents can be extracted by zeolites such as mordenite and clinoptilolite.[29]

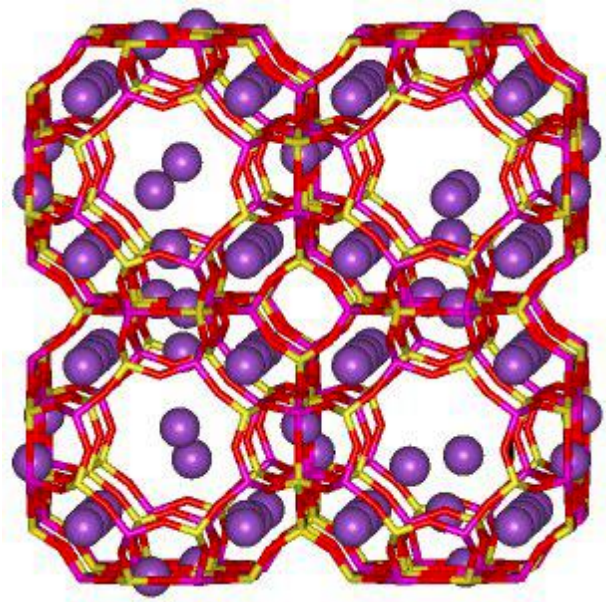

Figure 1.6. Extra-framework Na metal ion is shown in purple color in Zeolite 4A[30]

1.2.3.3.1 Cation exchange principle

According to Breck,[31] ion exchanges in zeolites are hard to understand fundamentally. They do not follow any easily discussed rules for the preference of ions. However, recently Jeffory and Bourtin et al. [32] computed the ion exchange isotherms using simulation studies. They considered the simple example between two univalent cations A^+ and B^+

$$A_{zeo}^{+} + B_{sol}^{+} \Longleftrightarrow A_{sol}^{+} + B_{zeo}^{+} \qquad 1.1$$

Where "zeo" and "sol" means ions present inside the zeolite and the solution. The cation mole fractions of i = A^+ or B^+ are expressed as:

$$X_{zeo}^{i} = \frac{n_{zeo}^{i}}{n_{zeo}^{total}}$$

$$X^{i}_{sol} = \frac{n^{i}_{sol}}{n^{total}_{sol}}$$

The cation exchange isotherm for equation 1.1 is obtained by plotting between X^{B}_{Zeo} Vs X^{B}_{sol}. The preference of one ion over the other can be understood from the below isotherm.

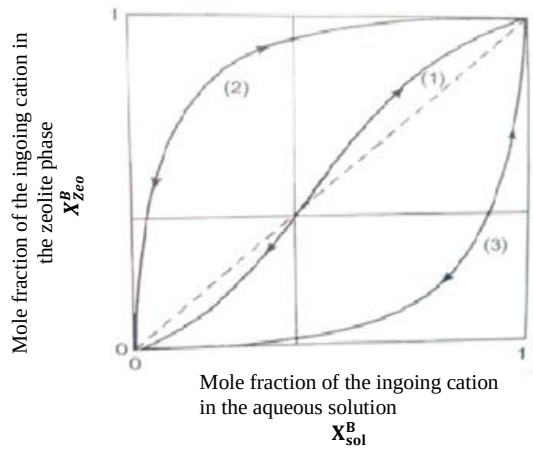

Figure 1.7. Cation exchange isotherm (adapted) [32]

The preferences of one ion over the another (A^{+} or B^{+}) can also be calculated as given by the selectivity factor: [32, 33]

$$\alpha^{B}_{A} = \frac{X^{B}_{Zeo}}{X^{B}_{sol}} \frac{X^{A}_{Zeo}}{X^{A}_{Zeo}}$$

1. When $\alpha^{B}_{A} = 1$, both A ion and B ion are equally preferred. Here the isotherm lies on the diagonal as represented by (1) in the Figure 1.7.
2. When $\alpha^{B}_{A} > 1$, ingoing B ion is preferred. Here the isotherm lies above the diagonal as represented by (2) in the Figure 1.7.
3. When $\alpha^{B}_{A} < 1$, outgoing A ion is preferred. Here the isotherm lies below the diagonal as represented by (3) in the Figure 1.7.

1.2.4 Different Framework Types

The different zeolite frameworks (Figure 1.9) used in this work is described below in detail.

1.2.4.1 LTA

"LTA" or "Linde-Type A" also called"Zeolite A" has an arrangement of larger polyhedra called α cages (supercages) which are connected to β cages through six-membered rings (Figure 1.8). The β cages are also called sodalite cages. The four-membered ring of the sodalite cage can also be linked through a four-membered prism as shown in Figure 1.8. It has a 3-dimensional pore structure running perpendicular to each other along X, Y and Z planes. The pore diameter is defined by an eight-member oxygen ring with an unobstructed diameter of 4.4 Å.

The free diameter in the central cavity is 11.4 Å. This can be reached through six 8-member oxygen rings. A unit cell of LTA has 12 $A1O_4$ and 12 SiO_4, and a total of 24 tetrahedra. So there are 12 negative charges which are balanced by cations. The unit cell formula for LTA is represented as: M x/n [($A1O_2$) x (SiO_2) y] .ZH_2O where y/x is equal to one. "n" is the valencey of the cation "M." The sodium form of zeolite A has a chemical formula of Na_{12} $(AlO_2)_{12}$ $(SiO_2)_{12}$. $27H_2O$.

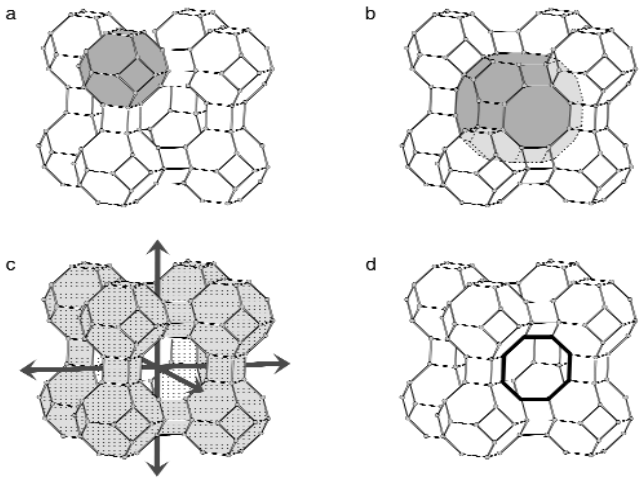

Figure 1.8. Pores in zeolite A (IZA code **LTA**)[34] (a) the sodalite cage (b) the α-cavity (c) the three-dimensional channel system, and (d) the 8-ring defining the 4.1Å effective channel width.

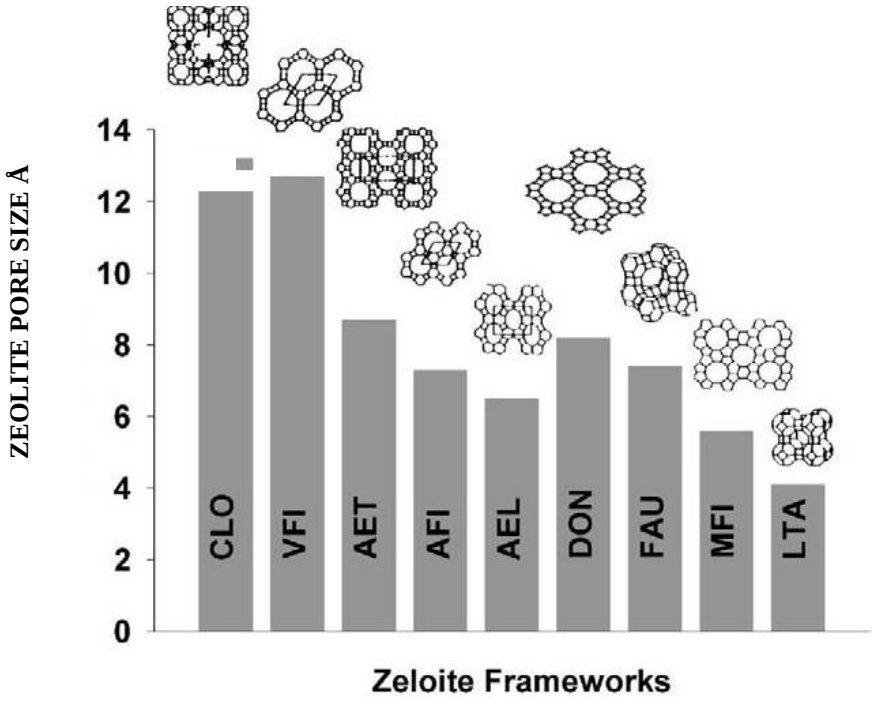

Figure 1.9. Comparison of pore sizes of different framework structures[47]

1.2.4.2 GIS

The framework-type code GIS is named after the mineral Gismondine. The framework structure is built entirely from six 4-member rings and four 8-member rings ($4^6\ 8^4$). GIS units are linked to form 8 ring aperture channels which have a free diameter of ~4 Å as shown in Figure 1.10. Two crankshaft chains and two 4-rings are connected in such a way that a channel with an 8-ring aperture (Figure 1.11) is formed. The secondary building units have an 8-member ring. The composite building unit has double crank shaft units (Figure 1.12) running parallel forming the channel system. It has a three-dimensional channel system. The chemical formula of the Na form of GIS is $Na_7Al_7Si_9O_{32}$•$9(H_2O)$ has a Si/Al ratio of 1.29.

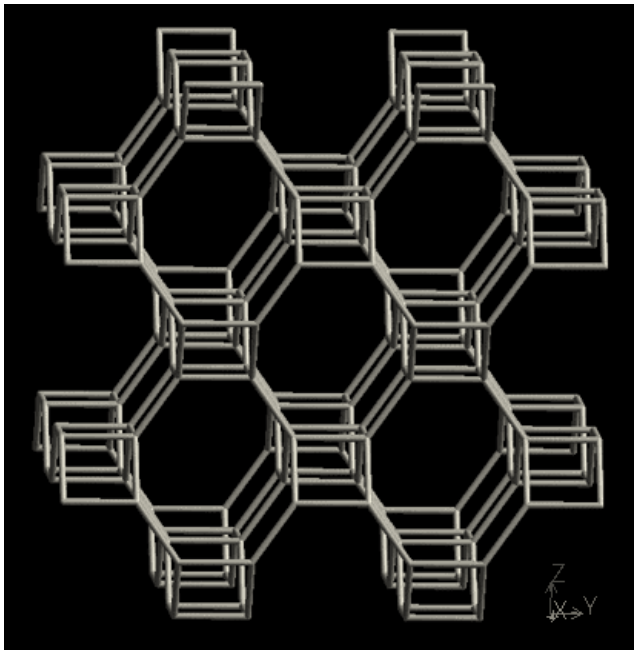

Figure 1.10. Structure of Gismondine Zeolite[35]

Figure 1.11. GIS double crank shaft chain as a composite building unit[29]

Figure 1.12. Double crank shaft chain in GIS zeolite[29]

1.2.4.3 RHO

The framework of zeolite RHO is composed of truncated cubo-octahedra or α-cages linked via double 8-rings. The α-cage is composed of 48 tetrahedral atoms with twelve 4-member rings, eight 6-member rings and six 8-member rings as shown in Figure 1.13. The three-dimensional framework of RHO is connected through double 8-member rings. There is a α-cage (Figure 1.14) at the centre of the cube. The channel is formed by an 8-ring aperture which has a free diameter of ~4 Å. It has a three-dimensional channel system. The chemical formula of RHO is $Na_{6.8}Cs_{3.0}[Al_{9.8}Si_{38.2}O_{96}].29\ H_2O$ with a Si/Al ratio of 3.9.

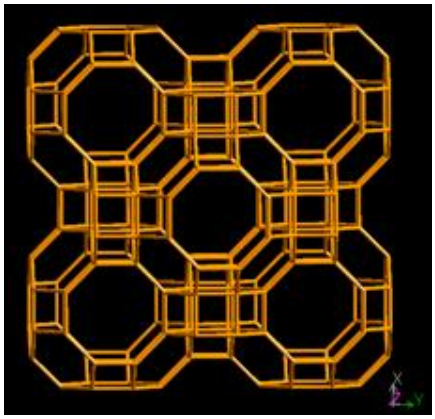

Figure 1.13. Zeolite RHO[29]

Figure 1.14. α cage in zeolite RHO[29]

1.2.4.4 FAU

In 1784, Barthelemy Faujas de Saint-Fond formulated a nice formalism based on the observations to identify zeolite in his book "mineralogy des volcanos". To honor him, a well known zeolite has been credited as "faujasite". Faujasite (FAU) finds most of its applications in the petroleum industry. Most gasoline is processed using faujasite-type zeolites. In the petroleum industry, an acidic form of faujasite zeolite Y[36] helps in high yield of gasoline and diesel fuel yield from crude oil. It helps in catalytic cracking by converting petroleum residue to low molecular weight olefins and gasoline. It is the second largest application of zeolites.

In this thesis, we will mainly concentrate on the faujasite zeolite (FAU LSX). The general formula is $M\ x/n\ [(A1O_2)\ x\ (SiO_2)\ y]\ .ZH_2O$ where X =Y= 96. This has the highest number of extra framework cations among the faujasites X and Y. The BET surface area of faujasites lies in the range between 500- 800 m^2/g.[1] The sodium form of FAU LSX has the chemical formula as $Na_{96}\ [Al_{96}Si_{96}O_{384}]$ ~235 H_2O. There are three faujasite type zeolites; LSX, X, Y and are differentiated based on Si/Al ratios. Faujasite with Si/Al ratio

= 1 is called LSX, between 1and 1.5 called the X, larger than 1.5 are called Y zeolites. The FAU framework (Figure 1.15) has AlO_4 and SiO_4 tetrahedra which are connected through oxygen linkage. These tetrahedra are otherwise called secondary building units (SBUs). They are as follows:

Four-member ring with 4 T (T= Al, Si) atoms in the corners of the ring and four oxygen atoms placed in the middle of each edge.

Six-member ring with 6 T atoms, in the six corners of the ring and six oxygen atoms placed in the middle of each edge. The six-member ring has a pore diameter of ~ 2.2 Å.

The supercage, central cavity or α cage has a free diameter of ~ 13.7 Å. Each supercage is connected to four other supercages through four β cages with their hexagonal faces. The supercage is composed of 18 four-member rings, 4 six-member rings and 4 twelve-member rings. The three-dimensional channels run parallel to the 12 ring window. The aperture to the channel is formed by the 12-member oxygen rings with a free diameter of ~ 7.4 Å.

Sodalite or β cage has eight 6-member rings and six-4 member rings. These cages are connected to each other through 6-member ring. The largest window of this cage is the six-oxygen ring with a free opening of 2.8 Å.

The unit cell of FAU has 192 tetrahedra which are arranged in sixteen 6 member rings, eight β cages and eight α cages. Faujasite zeolites have been synthesized with cations such as Li, Na, K, Rb, Cs, Ag, and Ca.[37]

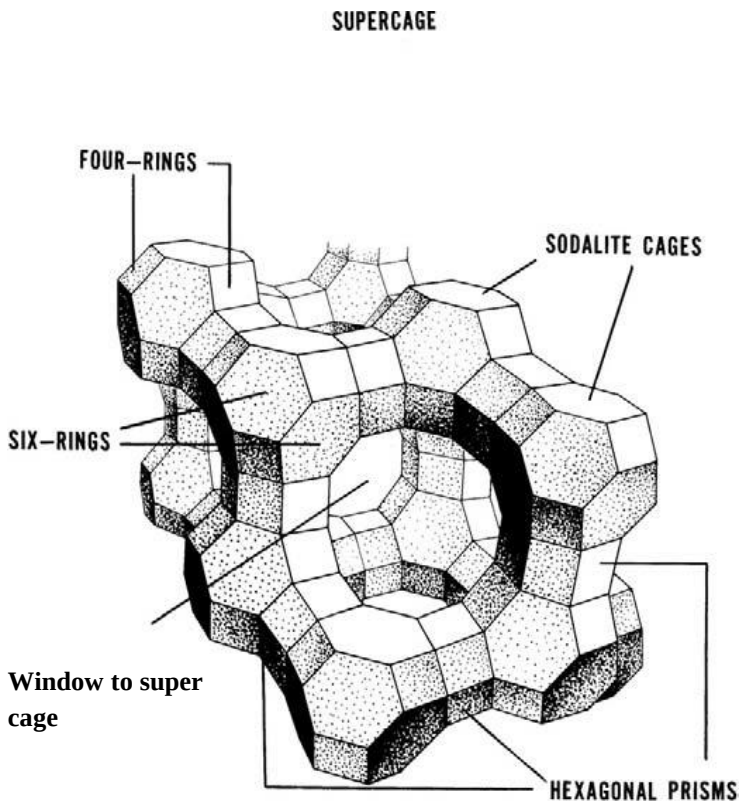

Figure 1.15. The framework of faujasite zeolite[37]

1.3. Literature Survey in gas separation in FAU zeolitic framework

The mobility of extra-framework cations and water molecules present in the zeolitic pores permits ion exchange, separation and removal of gases and solvents. The cations not only influence the pore size and volume, but also create an electric field inside the pores.[38] The extra-framework cations play a vital role in adsorption phenomena that occur in zeolites.[39, 40, 41] More fundamental studies on adsorptive separations are done in zeolites X, Y[42] containing monovalent cations with adsorbates like ethane,[43] CO_2,[44] water vapor.[45, 46] Zeolites are preferred in industrial gas separations for the uniformity and tunability of their pore sizes.[47,48, 49] Zeolites and charcoal have been used to accomplish the adsorption and separation of noble gases.[50, 51]

Li-LSX[1] is the best commercial adsorbent for the separation of N_2 from O_2. N_2 interacts much more strongly with Li^+ due to a significantly higher (electric field gradient-quadrupole) $\varphi_{\delta\ F\text{-}Q}$ potential. But, Ag Li- LSX is much better than Li-LSX for air separation.[52] This is due to a weak π-complexation bond formed between Ag and N_2. Maurin et al.[53] have reported the Ar adsorption in faujasite–X based on polarization energy. Both experimentally and theoretically, comparable numbers of studies were done on Kr and Xe separation by using metal organic framework[54, 55] materials.

1.4 Adsorption and gas separation

1.4.1 Adsorption –Definition

Adsorption is characterized by the accumulation of gas molecules to the surface of a solid. The adsorption process can be considered as a reversible condensation of gas molecules on the surface of the sample. During adsorption heat is evolved.

Adsorption is either classified as physisorption, where no chemical bonds are formed, or chemisorptions, which involves chemical bond formation. In the case of physisorption, there is a weak van der Waals force that holds the adsorbates on the surface of the adsorbent. As a result, the physisorption process can be reversed either by heating or lowering the pressure. Physisorption process takes place at low temperature and it decreases with increase in temperature. No activation energy is involved. And it occurs with low heats of adsorption in the range of 3-60 kJ/mol.

The gas separation techniques used are membrane-based, which depends on permeability of one gas over the other, cryogenic distillation based on the difference in the boiling

point of gases, and adsorption-based separation, which has advantages at different gas loadings as a function of pressure.[56,57] The synthesis of new adsorbents and the need of green separation have driven researchers to look for more on adsorptive separation.[58, 59]

1.4.2 Adsorbents and Adsorbates

A substance on whose surface adsorption takes place is called as an adsorbent. An adsorbate is a molecule adsorbed on the surface of the adsorbent. For an adsorbent to be used commercially, it should be available at an economical cost. In earlier days, adsorbents like silica and activated carbon were used. But with the development of synthetic zeolites, adsorption-based separation has reached a new milestone. According to Li et al.,[60] a promising adsorbent should have high adsorption capacity and good regenerability. Also, a better adsorbent should have large and uniform pore size and should interact well with the adsorbates. The strength of interaction between the adsorbents and the adsorbates depends on the surface characteristics of the adsorbent and also on the properties of adsorbates.

1.4.3 Properties of Kr and Xe

Both Kr and Xe belong to the noble gas family. They are chemically nearly inert and are non-polar in nature. Their atoms are symmetrical in nature. Both the kinetic diameter and polarizability (Table 1.1) of Xe are greater than of Kr.[61, 62]

Table 1.1. Physical Parameters of Kr and Xe[62]

Physical Parameters	Xe	Kr
Normal BP/K	165.01	119.74
Kinetic diameter/ Å	4.047	3.655
Polarizability $X10^{24}/cm^3$	4.044	2.484
Dipole moment $X10^{18}$/esu cm	0	0
Quadruple moment $X10^{18}/esu\ cm^2$	0	0

1.4.4 Adsorption isotherms

An adsorption isotherm is also known as equilibrium isotherm. It is a measure of the amount of adsorbate adsorbed on the adsorbent against relative pressures (P/P^0) at constant temperature. P stands for absolute pressure and P^0 stands for saturated pressure of the gas. Desorption occurs when the pressure is removed.

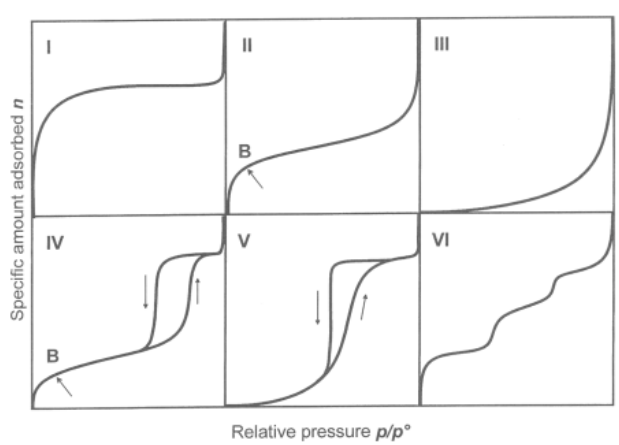

Figure 1.16. Classification of adsorption isotherms defined by IUPAC[63]

Six general types of isotherms have been classified by IUPAC[63] and the shapes of these characteristic isotherms are shown in Figure 1.16.

Type I: Microporous adsorbents (e.g., Zeolite and activated carbon)

Type II: Non porous solids. Multi layer adsorption occurs at higher P/P^0 (e.g., non porous alumina and silica)

Type III: Materials which have the weak interaction between the adsorbate and adsorbent (e.g., Graphite/water)

Type IV: Both mesoporous and non porous materials. Multi layer adsorption occurs. (e.g., Mesoporous Alumina and Silica)

Type V: Occurs in both microporous and mesoporous materials that have a weak interaction between the adsorbate and adsorbent (e.g., Activated carbon/water)

Type VI: Stepwise multi layer adsorption takes place on homogeneous surface materials (e.g., Graphite/Kr and NaCl/Kr)

Type I isotherms are typical of microporous solids where only monolayer adsorption occurs. It is common in zeolitic materials that we are interested in. These pores once filled in with the adsorbates have no more space for further adsorption to occur at higher loadings. The long plateau indicates small amount of multi layer adsorption in the exposed surface. Usually micropore filling occurs significantly at relatively low partial pressure $P/P^0 < 0.1$.

1.4.5 Factors affecting adsorptive gas separation

Factors that have to be considered for adsorptive gas separation are adsorbate–adsorbent interactions and the nature of the surface structure of adsorbents.

1.4.5.1 Adsorbate and Adsorbent interactions

The total potential between the adsorbate molecules and the adsorbent is the sum of the adsorbate-adsorbate and the adsorbate-adsorbent interaction potentials given as: [58, 64]

$$\varphi_{total} = (\varphi_{adsorbate\text{ - }adsorbate}) + (\varphi_{adsorbate\text{ - }adsorbent}) \qquad 1.2$$

The adsorbent has only a secondary effect on the adsorbate–adsorbate interaction. For this reason, only the second term, adsorbate–adsorbent potential is focused and referred as φ.[58] For physical adsorption, the adsorbate–adsorbent potential is:

$$\varphi = \varphi_D + \varphi_R + \varphi_P + \varphi_{F\text{-}\mu} + \varphi_{\delta\ F\text{-}Q} \qquad 1.3$$

Where φ_D is the dispersion potential and φ_R is the close-range repulsion potential. The terms φ_D , φ_R are common in all adsorbate and adsorbent systems.[65] Polarization energy φ_P, field-dipole interaction $\varphi_{F\text{-}\mu}$ and field gradient-quadrupole interaction $\varphi_{\delta\ F\text{-}Q}$ arise due to charges. The term $\varphi_{P\ is}$ refers to the polarization of the adsorbate molecule by the electric field on the surface of the adsorbents. The terms $\varphi_{F\text{-}\mu}$, $\varphi_{\delta\ F\text{-}Q}$ are non-zero when the adsorbate molecule has a permanent dipole moment or quadrupole moment.

The term $\varphi_{adsorbate - adsorbate}$ arises due to the interaction between the adsorbate molecules. It is present even if the adsorbate molecules are non- polar and the adsorbent surface does not have an electric field. However this contribution is zero at low coverages of adsorbents by the adsorbates. At high coverages it can sometimes be seen with a visible increase in the heats of adsorption.

It can be shown that the heat of adsorption at low coverage is related[3] to the adsorbate–adsorbent interaction potential (φ) by

$$\Delta H = \varphi_{total} - RT + F(T) \qquad 1.4$$

Where ΔH = heat of adsorption and F(T) is related to the vibration and translational energies of the adsorbate molecule. As F(T) and RT are small at ambient temperature, ΔH becomes

$$\Delta H = \varphi_{total} \qquad 1.5$$

1.4.5.2 Surface structure of adsorbents

Surface structure of natural zeolites is heterogeneous in nature as they have different gas adsorption sites. Hence they have different gas selectivities on their different surfaces.[66] Highly dealuminated zeolites have more homogeneous surface and consequently exhibit hydrophobicity and preferably adsorb non-polar molecules.[67] This favors dispersion interaction rather than the polar attraction as the electric field is decreased on the surface area of zeolites.

1.5. Heat of Adsorption using Clausius-Clapeyron equation

For physisorption to be a spontaneous thermodynamic process, ΔG has to be negative. Also the translational degree of freedom is lost during the deposition of gas phase adsorbate on the adsorbent. So ΔS is negative. As $\Delta G = \Delta H - T\Delta S$, ΔH is negative for physisorption process to occur. This ΔH or the heat evolved is referred as the heats of adsorption. The heats of adsorption is the measure of strength of interaction and adsorption affinity of adsorbate for adsorbent. The isosteric heats of adsorption in this work were obtained from the adsorption data collected at different temperatures by using the Clausius-Clapeyron equation: [58]

$$\Delta_{ad} H^{o} = R \{[\partial \ln p]/ [\partial (1/T)]\}_{\theta} \qquad 1.6$$

Where "R" is the universal gas constant, θ is the fraction of adsorbed sites at pressure p and temperature T respectively. A plot of ln p against 1/T gives a straight line with a slope. The slope multiplied by R gives $\Delta_{ad}H^{o}$.

CHAPTER 2

EXPERIMENTAL PROCEDURES

The experimental procedures adapted for the synthesis of zeolites in this thesis and the corresponding ion exchange procedures are discussed in detail in section 2.1 and 2.2. The material characterization performed by Powder X-ray diffraction studies and the elemental analysis done by Inductively Coupled Plasma Atomic Emission Spectroscopy are outlined in section 2.3.1 and 2.3.2. Finally, adsorption isotherm measurement is explained in section 2.4.

2.1. Material Synthesis

In this thesis, the zeolitic materials used as adsorbents like FAU LSX, LTA, RHO, GIS were synthesized hydrothermally by adapting the procedure from "Verified Synthesis of Zeolitic Materials" by H. Robson.[1]

2.1.1. LTA -Synthesis procedure

About 80 ml of deionized water and 0.728 g of NaOH (supplied by Alfa Aesar) were mixed gently until the NaOH completely dissolved. The solution was divided into two equal portions in polypropylene bottles. To the first portion, 8.267 g of sodium aluminate (supplied by Spectrum) was mixed gently until the capped bottle was clear. To the second portion, 15.47 g of sodium silicate (supplied by Alfa Aesar) was mixed gently in another capped bottle until clear. The second portion was added to the first portion, resulting in a thick gel. This gel was capped tightly and mixed vigorously by hand for 10 minutes in a polypropylene bottle with equal intervals. This was placed in an oven at 100°C for four hours. The product was removed from the oven and cooled at 25°C. The product was

washed with one liter of deionized water and filtered by suction filtration. The final product was obtained after heating in a preheated oven at 110°C overnight.

2.1.2. RHO - Synthesis Procedure

About 7.89 g of deionized water, 1.360 g of 18-C-6 (supplied by Alfa Aesar) and 1.810 g of CsOH (supplied by Alfa Aesar) and 0.597 g of NaOH (supplied by Alfa Aesar) were stirred until dissolved in a polypropylene bottle. To this, 1.823 g of sodium aluminate (supplied by Alfa Aesar) was added and stirred until they were uniformly mixed. To this, 20.05 g of silica sol (supplied by Aldrich chemical) was added and stirred well to form a gel. The gel pH was found to be 13.28. The gel was stirred continuously with a magnetic stirrer for 24 hours. This was transferred to a PTFE-lined 120 ml stainless steel auto clave and placed in a preheated oven at 110°C for 192 hours. The product obtained was washed with deionized water, until the pH was ~ 10.0 and filtered by vacuum filtration until it was dried. The final product, RHO Na Cs was obtained by further drying the sample in a preheated oven at 60° C over night.

2.1.3. GIS - Synthesis Procedure

About 43.85 ml of deionized water and 5.212 g of NaF were stirred together in a polypropylene bottle to form a slurry for 30 minutes by using a magnetic stirrer. To this about 6.092 g of pre washed "kaolin" ($Al_2Si_2O_7.2H_2O$, supplied by Alfa Aesar) was added and mixed thoroughly by using a stirrer for 10 minutes. This was heated in a preheated oven at 95° C for 60 days. (Note: The Kaolin used was first placed in deionized water overnight, filtered and dried.) After 60 days, the mixture was taken out of the oven and washed thoroughly with 500 ml of deionized water. This was further exchanged

twice with 50 ml of 0.1M NaCl solution at one hour intervals. This was washed again with distilled water, until the pH was adjusted to 10.50. The product obtained was dried in a preheated oven at 85°C for 24 hours.

2.1.4. FAU LSX - Synthesis Procedure

About 7.58 ml of deionized water and 5.594 g of sodium aluminate (supplied by Alfa Aesar) were stirred to dissolve in a polypropylene bottle. In another polypropylene bottle, about 17.52 ml of water, 5.394 g of KOH (supplied by JT Baker) and 5.454 g of NaOH (supplied by Alfa Aesar) were stirred for 3 minutes and dissolved. The above 2 mixtures were mixed thoroughly for 20 minutes using a stirrer which resulted in a turbid solution. To this about 18 ml of H_2O and 11.491 g of sodium silicate solution (supplied by Johnson Matthey Catalog Company) were mixed thoroughly for 15 minutes. This resulted in a gel which was placed in an oven at 70° C without stirring for 3 hours. After this incubation period, it was again heated in an oven at 95° C for 2 hours. The product obtained was taken out and diluted with 50 ml of water. This was washed with 500 ml of 0.01M NaOH solution and filtered by vacuum filtration. The final product was obtained after heating in a preheated oven at 100°C overnight.

2.2. ION EXCHANGE

The above as synthesized zeolites were further ion-exchanged with cations like Li^+, Na^+, K^+, Rb^+, Cs^+, Ca^{2+} with LSX zeolites and Ca^{2+} ion with LTA, RHO, GIS zeolites respectively. The cation exchange principle has already been discussed in section 1.2.3.3.1.

2.2.1. LTA Ca

The ion exchange procedure was partially adapted from "Diffusion in ion-exchanged clinoptilolites" by Ackley and Yang et al.[2] Approximately 2 g of the above as synthesized LTA Na was weighed and placed in a polypropylene bottle with 20 ml of 0.1 M $CaCl_2$ solution[3] which was prepared in the lab. The bottle was capped and stirred at 25°C for 3 hours. This solution was decanted by centrifuging for 3 times followed by washing with ~ 20 ml of water each time. The zeolite settled at the bottom of the centrifuge tube and the filtrate was decanted. This procedure was repeated 9 times by replacing with 20 ml of fresh 0.1M $CaCl_2$ solution each time. This solution was washed with ~750 ml of deionized water and filtered by vacuum filtration. Finally the product obtained was dried in a preheated oven at 100° C over night. Doing further ICP analysis on this product confirmed that LTA Na was effectively 100% ion-exchanged to LTA Ca.

2.2.2. RHO Ca

The ion exchange procedure was adapted partially from Ackley et al.[2] About ~1 g of as synthesized RHO Na Cs was weighed and placed in a polypropylene bottle with 10 ml of 1.0 M $CaCl_2$ solution[3] which was prepared in the lab. The bottle was capped and stirred at 50° C for 3 hours. This solution was decanted by centrifuging for 3 times followed by washing with ~ 10 ml of water each time. The zeolite settled at the bottom of the centrifuge tube and the filtrate was decanted. This procedure was repeated 12 times by replacing with 10 ml of fresh 1.0 M $CaCl_2$ solution each time. This solution was washed with ~750 ml of deionized water and filtered by vacuum filtration. Finally the product

obtained was dried in a preheated oven at 100° C over night. Doing further ICP analysis on this product confirmed that RHO Na Cs was 86% ion-exchanged to RHO Ca.

2.2.3. GIS Ca

About ~1 g of as synthesized GIS Na was weighed and placed in a polypropylene bottle with 10 ml of 1.0 M $CaCl_2$ solution, [3] which was prepared in the lab. The ion exchange procedure was partially adapted from Ackley et al.[2] The bottle was capped and stirred at 50° C for 3 hours. This solution was decanted by centrifuging for 3 times, followed by washing with ~ 10 ml of water each time. The zeolite settled at the bottom of the centrifuge tube and the filtrate was decanted. This procedure was repeated for 7 times by replacing with 10 ml of fresh 1M $CaCl_2$ solution each time. This solution was washed with ~750 ml of deionized water and filtered by vacuum filtration. Finally, the product obtained was dried in a preheated oven at 100° C over night. Doing further ICP analysis on this product confirmed that GIS Na was 92% ion-exchanged to GIS Ca.

2.2.4. FAU LSX Ca

The procedure was partially adapted from "Multicomponent Ion Exchange in Zeolites"[4] by Franklin, Townsend et al. About ~2 g of synthesized FAU Na was weighed and placed in a polypropylene bottle with 20 ml of 0.1M $CaCl_2$ solution which was prepared in the lab. The bottle was capped and stirred at 25° C for 3 hours. This solution was decanted by centrifuging for 3 times followed by washing with ~ 10 ml of water each time. The zeolite settled at the bottom of the centrifuge tube and the filtrate was decanted. This procedure was repeated for 10 times by replacing with 20 ml of fresh 0.1M $CaCl_2$ solution each time. This solution was washed with ~750 ml of deionized water and

filtered by vacuum filtration. Finally the product obtained was dried in a preheated oven at 100° C over night. Doing further ICP analysis on this product confirmed that FAU Na was completely ion-exchanged to FAU Ca.

2.2.5. FAU LSX Li

The procedure was partially adapted from Townsend et al.[4] About ~2 g of synthesized FAU Na was weighed and placed in a polypropylene bottle with 20 ml of 0.1M LiCl solution[3] which was prepared in the lab. The bottle was capped and stirred at 25°C for 3 hours. This solution was decanted by centrifuging for 3 times followed by washing with ~ 10 ml of water each time. The zeolite settled at the bottom of the centrifuge tube and the filtrate was decanted. This procedure was repeated 11 times by replacing with 20 ml of fresh 0.1M LiCl solution each time. This solution was washed with ~750 ml of deionized water and filtered in a vacuum pump. Finally the product obtained was dried in a preheated oven at 100°C over night. Doing further ICP analysis on this product confirmed that FAU Na was 83 % ion-exchanged to FAU Li.

2.2.6. FAU LSX Na

This procedure was partially adapted from Townsend et al.[4] About ~2 g of as synthesized FAU LSX was weighed and placed in a polypropylene bottle with 20 ml of 1.0 M NaCl solution[3] which was prepared in the lab. The bottle was capped and stirred at 50° C for 3 hours. This solution was decanted by centrifuging 3 times followed by washing with ~ 10 ml of water each time. The zeolite settled at the bottom of the centrifuge tube and the filtrate was decanted. This procedure was repeated 7 times by replacing with 10 ml of fresh 1.0 M NaCl solution each time. This solution was washed with ~750 ml of

deionized water and filtered by vacuum filtration. Finally the product obtained was dried in a preheated oven at 100°C over night. Doing further ICP analysis on this product confirmed that FAU Na K was 100% ion-exchanged to FAU Na.

2.2.7. FAU LSX K

The procedure was partially adapted from Townsend et al. [4] About ~2 g of synthesized FAU Na was weighed and placed in a polypropylene bottle with 20 ml of 0.1M KCl solution[3] which was prepared in the lab. The bottle was capped and stirred at 25°C for 3 hours. This solution was decanted by centrifuging 3 times followed by washing with ~ 10 ml of water each time. By doing so, the zeolite got settled at the bottom of the centrifuge tube and the filtrate was decanted. This procedure was repeated 11 times by replacing with 20 ml of fresh 0.1M KCl solution each time. This solution was washed with ~750 ml of deionized water and filtered by vacuum filtration. Finally, the product obtained was dried in a preheated oven at 100° C over night. Doing further ICP analysis on this product confirmed that FAU Na was ~82 % ion-exchanged to FAU K. This was further ion-exchanged to 100% by treating ~1 g of ~82% ion-exchanged FAU K in 10 ml of 1M KCl at 50° C for 5 times.

2.2.8. FAU LSX Rb

The procedure was partially adapted from Townsend et al.[4] About ~2 g of synthesized FAU Na was weighed and placed in a polypropylene bottle with 20 ml of 0.1M RbCl solution which was prepared in the lab.[3] The bottle was capped and stirred at 25°C for 3 hours. This solution was decanted by centrifuging 3 times followed by washing with ~ 10 ml of water each time. The zeolite settled at the bottom of the centrifuge tube and the

filtrate was decanted. This procedure was repeated 10 times by replacing with 20 ml of fresh 0.1M RbCl solution each time. This solution was washed with ~750 ml of deionized water and filtered by vacuum filtration. Finally, the product obtained was dried in a preheated oven at 100° C over night. Doing further ICP analysis on this product confirmed that FAU Na was ~34 % ion-exchanged to FAU Rb.

2.2.9. FAU LSX Cs

The procedure was partially adapted from Townsend et al.[4] About ~2 g of synthesized FAU Na was weighed and placed in a polypropylene bottle with 20 ml of 0.1M CsCl solution[3] which was prepared in the lab. The bottle was capped and stirred at 25° C for 3 hours. This solution was decanted by centrifuging 3 times followed by washing with ~ 10 ml of water each time. The zeolite settled at the bottom of the centrifuge tube and the filtrate was decanted. This procedure was repeated 11 times by replacing with 20 ml of fresh 0.1M CsCl solution each time. This solution was washed with ~750 ml of deionized water and filtered by vacuum filtration. Finally the product obtained was dried in a preheated oven at 100°C over night. Doing further ICP analysis on this product confirmed that FAU Na was ~50 % ion-exchanged to FAU Cs.

2.3. Material Characterization

2.3.1. X ray powder diffraction

Crystallinity and phase purity of the zeolites FAU LSX, LTA, RHO, GIS samples were identified from their X-ray diffraction patterns. All the samples (as-synthesized and ion-exchanged) were characterized on a Bruker D8 Discover diffractometer for phase purity and identification.

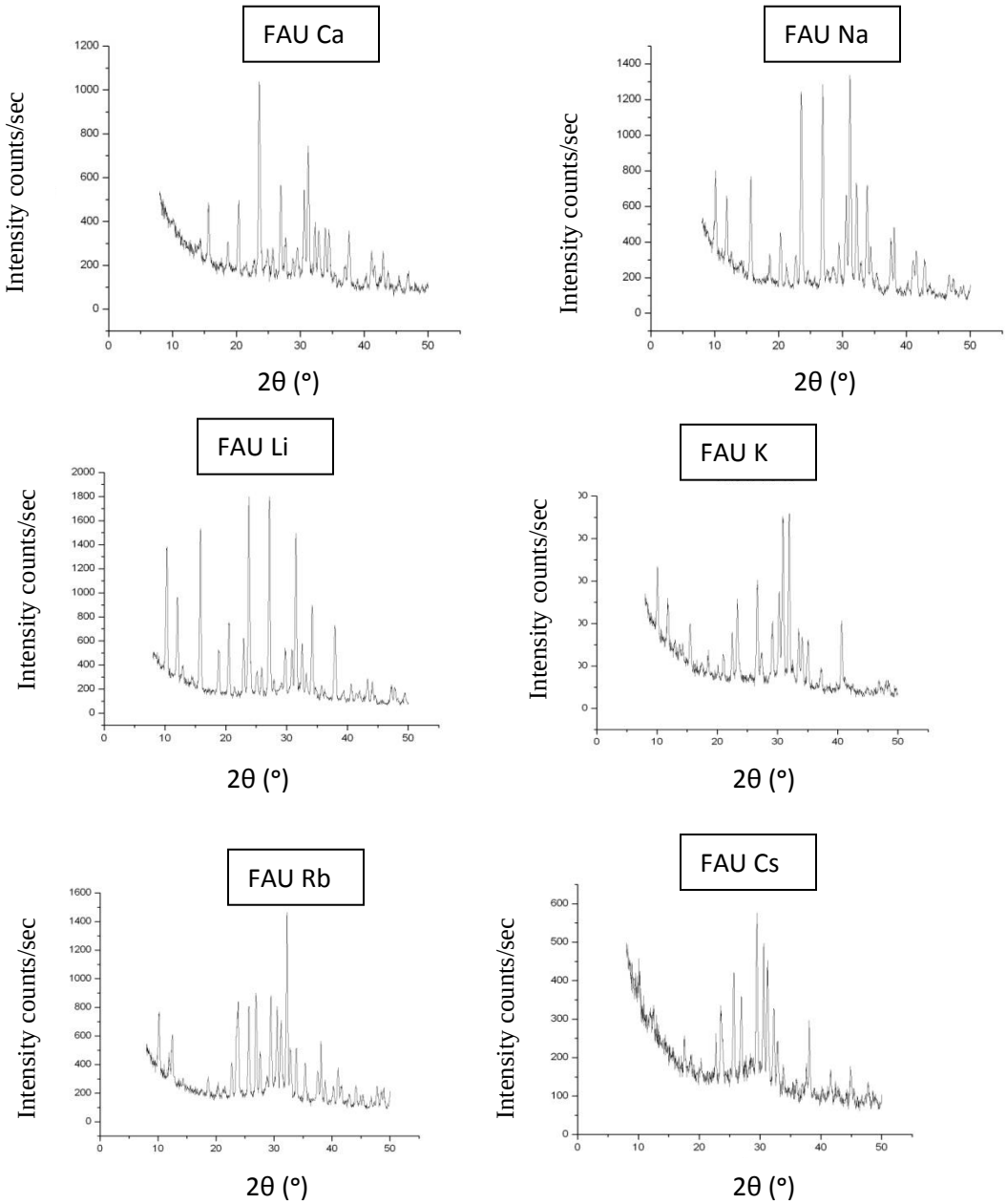

Figure 2.1. X-ray diffraction patterns of FAU LSX zeolites

The diffraction patterns of the materials showed the reflections in the range 5-35° typical of zeolites. The structures of the zeolites were retained even after the cation exchange.

2.3.2. Elemental analysis

Elemental analysis for inorganic ions as well as Si/Al ratios in all of the above discussed zeolites was determined by inductively coupled plasma-atomic emission spectroscopy (ICP-AES). All the standard solutions used in the analysis were prepared in the lab.[3] The reagents HF, HCl, HNO_3, H_3BO_3 were supplied by Aristar BDH, JT Baker, Aristar plus and Alfa Aesar respectively.

The zeolites have challenges in sample preparation for analyzing them by using ICP AES. The most difficult step is dissolving the sample into solution form. According to Chao, Chen et al,[5] zeolites can be dissolved through acid digestion process when done under pressure. HF in combination with aqua regia was tested for dissolving the zeolites. However, there were two problems to be considered while dissolving zeolites by using the acid digestion procedure. First, the loss of Si as H_2SiF_6 during digestion and, second the presence of excess HF during the decomposition procedure. This might cause a corrosive effect on the nebulizer and spray chamber which are made out of glass in ICP instrument. In order to get a complete recovery of Si and to avoid the corrosive effect of excess HF on glass, Chao et al. suggested digestion of zeolites like NaX, NaY, NaA zeolites by decomposing them in a mixture of aqua regia and HF (0.1 to 0.5 ml) for 0.1 g of zeolite. H_3BO_3 was further added which reacts with excess HF and forms fluoroboric acid:

$$B(OH)_3 + 4\ HF \rightarrow H_3O^+ + BF_4^- + 2\ H_2O$$

Analytical procedure for preparing zeolite samples in the ICP analysis were adapted from Chao et al.[5] Approximately, 0.04 g of zeolite was weighed in a 23 ml Teflon vessel.

About 1.2 ml of conc. HCl and 0.4 ml of conc. HNO_3 were added to it and placed in a liquid nitrogen dewar for cooling. To this, about 0.070 ml of HF was added and the Teflon vessel was immediately sealed in an autoclave and heated at 150° C for 4 hours. After being cooled to room temperature, about 0.2 g of H_3BO_3 was added to neutralize the excess HF.

In all our experimental procedures, we could dissolve zeolite only after adding 0.070 ml of HF rather than 0.2 ml as suggested by Chao et al.[5] Addition of 0.2 ml of HF resulted in the precipitation of insoluble aluminum fluorides. So, based on stoichiometric calculation and after several numbers of trials, we decided to add 0.070 ml of HF. The resulting solution was diluted with water and transferred in a 100 ml polypropylene bottle. Finally the resulting zeolite solution was analyzed for the determination of Al, Si, and other inorganic ions using ICP AES. Their unit cell compositions and % ion-exchanged are given in the Table 2.1.

2.3.2.1. Experimental and apparatus

A Thermo Scientific inductively coupled plasma atomic emission spectrometer was used. The instrumental specifications and operating conditions used in this study are listed in Table 2.2. A pressure digestion system which comprises a 23 ml PTFE vessel and a thermostatically-controlled heating block was used for the digestion of the zeolite samples.

Teflon, polyethylene and polypropylene containers were used throughout the work. They were cleaned by immersing in conc. HNO_3 overnight and washing successively with deionized water. All chemicals used were of analytical grade. High-purity water

produced by reverse osmosis and demineralization processes was used. Stock solutions used to prepare the standards in ICP-AES for elemental analysis are discussed in Appendix 1.

Table 2.1. Unit cell composition, % ion exchange and Si/Al ratio determined from ICP-AES

Adsorbent	Unit cell composition	% Ion exchange	Si/Al
LTA Ca	$Ca_{7.68}\ Al_{11.82}\ Si_{12.18}\ O_{48}$	100%	1.03
RHO Ca Cs	$Na_{0.14}\ Cs_{2.67}\ Ca_{4.42}\ Al_{10.17}\ Si_{37.83}\ O_{96}$	86%	3.72
GIS Ca	$Na_{0.40}\ Ca_{1.81}\ Al_{3.9}\ Si_{11.1}\ O_{30}$	92%	2.85
FAU LSX Ca	$Ca_{61.29}\ Al_{95.05}\ Si_{96.95}\ O_{384}$	100%	1.01
FAU LSX Li	$Li_{80.23}\ Na_{18.44}\ Al_{94.25}Si_{97.75}\ O_{384}$	85%	1.04
FAU LSX Na	$Na_{102.52}Al_{95.52}Si_{96.48}\ O_{384}$	100%	1.01
FAU LSX K	$K_{97.41}\ Al_{94.58}Si_{97.42}\ O_{384}$	100%	1.03
FAU LSX Rb	$Na_{44.25}\ Rb_{32.56}\ Al_{94.58}\ Si_{97.42}\ O_{384}$	34%	1.03
FAU LSX Cs	$Na_{46.23}\ Cs_{51.13}\ Al_{100.52}\ Si_{91.48}O_{384}$	51%	0.91

Table 2.2. ICP AES instrumental specifications

ICP AES	
Manufacturer	Thermo Scientific
Model	iCAP 6500 Duo
Spectrometer	Simultaneous echelle type, 52.91 grooves/mm ruled grating,383 mm effective focal length, 166-847 nm wavelength range
RF generator	27.12 MHz
RF Power	1150 W
Nebulizer Gas (Argon)	0.51 L/min
Auxiliary Gas (Argon)	0.5 L/min
Plasma Gas (Argon)	12 L/min
Nebulizer Type	Meinhard concentric glass nebulizer
Pump Flow	50 rpm

2.4 Adsorption isotherm measurement

Gas adsorption isotherms were measured using a Micromeritics[6] ASAP 2020 instrument fitted with a helium cryostat manufactured by Cold Edge technologies. In a typical experiment, about 100 mg of each sample was ground, placed into a calibrated tube, and activated under vacuum at ~ 150° C for 18- 24 hours. The activated sample mass was then determined by reweighing the entire sample tube. The BET surface area was calculated from the N_2 adsorption isotherm at 77 K using the methods described by Walton and Snurr[7] and is comparable to those reported for all the fully activated zeolite samples.

Following each measurement, the samples were removed from the cryostat and heated under vacuum at 100° C for an hour to remove all the adsorbed gases then replaced into the cryostat for the next measurement. Approximately one hour was given in the cryostat prior to starting the measurement to allow for thermal equilibration of the sample and the cryostat. Adsorption isotherms were collected over a range of 0 to 700 mmHg with a fixed volumetric dose of 5 cm^3/g and long equilibration times at each dose.

Adsorption isotherms for Xe were collected at the following temperatures: 280 K, 290 K, and 300 K and for Kr at 230 K, 240 K, and 250 K. Type I isotherms were observed for all samples. As hysteresis in these isotherms would indicate that equilibrium has not been reached, we measured desorption isotherms in all cases and only used data that had negligible hysteresis. Heat of adsorption calculations for each gas were carried out by applying the Clausius-Clapyeron equation (equation 1.6) to isotherms collected at different tempetaures using Micromeritics software.[6]

CHAPTER 3

RESULTS AND DISCUSSION

Our focus is on finding a suitable adsorbent for the separation of Kr from Xe using zeolites. Zeolites have several advantages in gas separation; they are stable to very high temperature as well as tolerant to acidic and corrosive environments. Many zeolites can be synthesized inexpensively and through environmental friendly ways. Unlike most MOF's, their production does not usually require expensive organic ligands or transition metals.

Among commercial gas separation processes, pressure swing adsorption (PSA) is preferred for small-scale needs and low-energy consumption.[1] In this thesis, we have determined the adsorption isotherms of Kr and Xe with the synthesized zeolites in the lab using gas adsorption studies and calculated their heats of adsorption in order to examine their sorbate-sorbent interactions. Finally, we have compared the differences in their heats of adsorption to find out a suitable sorbent that has high selectivity of one gas over the other.

We have carried out the adsorption measurements in two sets of zeolites. First, we are comparing same zeolite framework (FAU LSX) but with different alkali cations. A promising adsorbent with high surface area and large pore size would allow easier interaction of non polar adsorbate with the interior of an adsorbent.[2] Second, we have compared different zeolite frameworks like LTA, FAU LSX, RHO and GIS with same extra-framework cation (Ca^{2+}). The zeolitic frameworks that we have chosen have pore

diameters comparable to the kinetic diameter of Kr and Xe. We hypothesize that this may help in discriminating one atom over the other based on size exclusion.

Table 3.1. As-synthesized zeolites in Lab

ZEOLITES	ION	RING TYPE	PORE DIAMETER
FAU LSX	Na & K	12-MR	7.4 Å
GIS	Ca	8-MR	4.5 Å
LTA	Na	8-MR	4.1 Å
RHO	Na & Cs	8-MR	3.6 Å

3.1. Adsorption isotherm measurement

An adsorption isotherm is a measure of the amount of gas adsorbed on the adsorbent against relative pressure at constant temperature. A typical adsorption isotherm measurement has already been discussed in section 2.4 of this work. Adsorption measurements are carried out for each sample with Kr at 230 K, 240 K, and 250 K and for Xe at 280 K, 290 K and 300 K. The corresponding adsorption isotherms are represented in Figure 3.1. In all the isotherms shown, as the temperature has increased the adsorbed amount has decreased since adsorption is an exothermic process. Subsequent to each adsorption measurement, desorption is measured. A negligible hysteresis between adsorption and desorption confirms that equilibrium is achieved at each adsorption/desorption point.

3.2 Gas adsorption studies of Kr and Xe using FAU LSX zeolite with different alkali cations

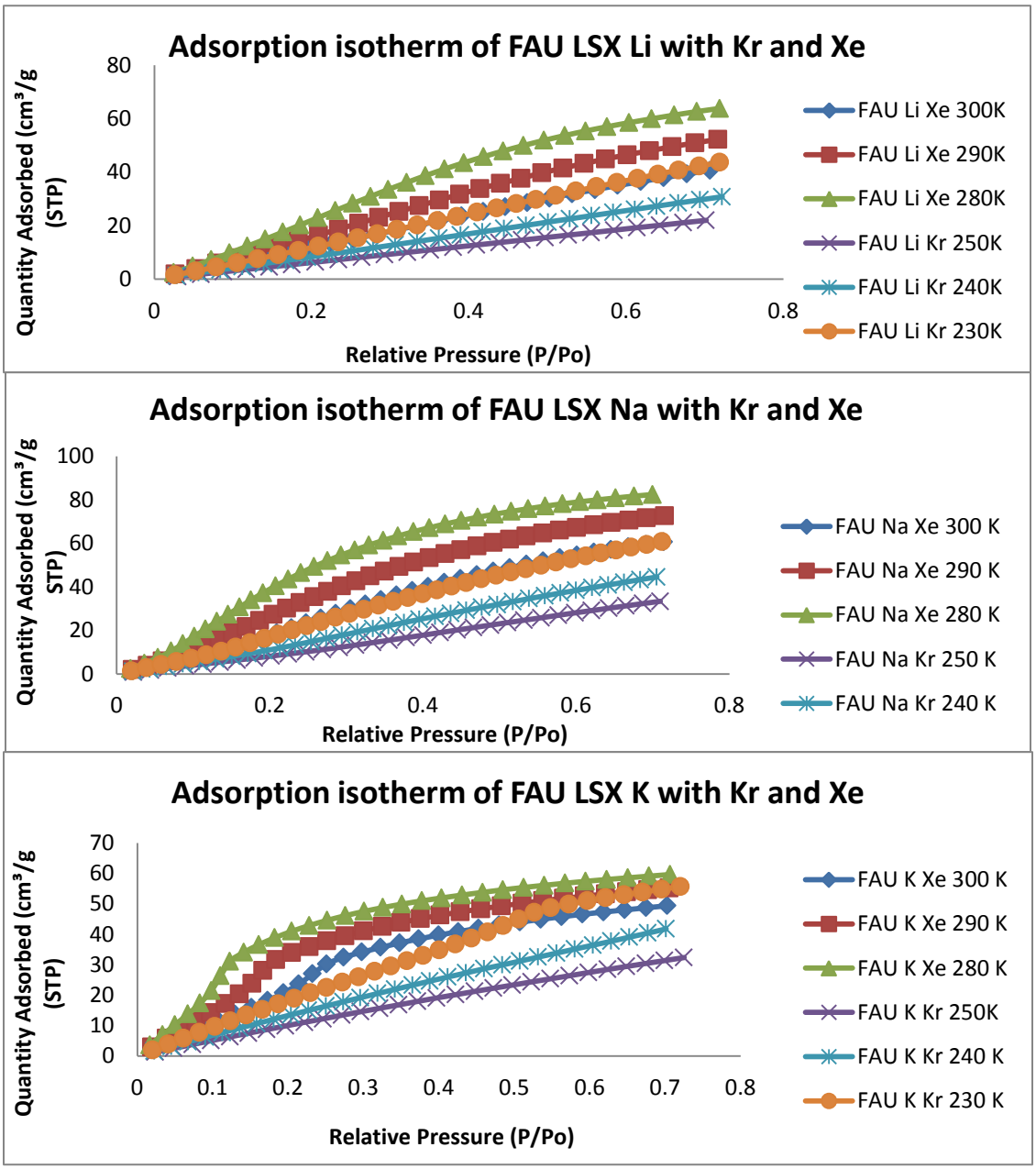

Figure 3.1. Kr and Xe adsorption isotherms in the alkali metal ion-exchanged FAU LSX at different temperatures.

From the Figure 3.1, we see that we have not reached the maximum adsorption capacities in all of the ion-exchanged FAU LSX zeolites by 700 mm Hg limit due to the pressure limit of the instrument (FAU LSX Rb and Cs adsorption isotherm are given in Appendix 2). This can be clearly observed with the adsorption curves still exhibiting a positive slope. The equilibrium adsorption capacity for Kr and Xe in alkali metal ion-exchanged LSX at 700 mm Hg is given in Appendix 2. We have also calculated the number of atoms per supercage in FAU LSX zeolites at 700 mm Hg in Table 3.2.

Table 3.2. Kr and Xe atoms per supercage at 700 mm Hg in FAU LSX

Adsorbate	Kr			Xe		
Adsorbent	230K	240K	250K	280K	290K	300K
Li LSX	3.03	2.20	1.67	4.31	3.59	2.95
Na LSX	4.65	3.41	2.56	6.31	5.56	4.65
K LSX	4.74	3.55	2.75	5.08	4.70	4.20
Rb LSX*	2.87	2.31	1.88	3.08	2.74	2.41
Cs LSX*	3.67	2.93	2.35	3.31	2.91	2.52

*NOTE: Rb and Cs samples are only 34% and 51% ion-exchanged. Li is 85% ion-exchanged.

The framework of zeolite FAU LSX has a large super cage with 12-member ring window with a pore diameter of 7.4 Å. The kinetic diameter of Kr and Xe are 3.655 Å and 4.047 Å. So the entry of both Kr and Xe into the 12-member ring supercage is unhindered. But the adsorption of Kr and Xe into the supercages is not similar for all the alkali cations in FAU LSX. In our study we see that, (Table 3.2) with all the cations comparatively more

Xe atoms are adsorbed than Kr. This is due to the higher polarizability of Xe than Kr. The higher polarizability of Xe influences higher van der Waal's interaction with the cation. With smaller cations comparatively more Kr and Xe atoms are adsorbed than larger cations like Rb and Cs. At the same time, it has to be noted that both Rb and Cs are only partially ion-exchanged. Also, we have not measured the adsorption isotherms with all of these adsorbents to the maximum loadings due to our instrumental limitation. Hence we cannot account for the exact order of preference of atoms in these zeolites.

3.2.1. Heats of adsorption in FAU LSX zeolites with different alkali cations

One of the critical parameters to assess the separation potential of a material is heats of adsorption.[3] This can be calculated by applying the Clausius-Clapyeron Equation (Equation 1.6) to equilibrium adsorption isotherms obtained at different temperatures. The heats of adsorption for the alkali ion-exchanged FAU LSX zeolite is calculated for Kr by using adsorption isotherms measured at 230 K, 240 K and 250 K and for Xe, adsorption isotherms are measured at 280 K, 290 K and 300 K.

In order to evaluate the strength of adsorbate-adsorbent interactions in FAU LSX zeolites, the differential enthalpies of adsorption at zero coverage $\Delta_{ads}h_{\theta = 0}$ are then extracted from the graph by extrapolating the curves to zero coverage. The results are summarized in Table 3.3. The differential heats of adsorption calculated at zero coverage for the adsorbates (Kr and Xe) and the alkali ion-exchanged FAU LSX zeolite are related to selectivity of one gas over the other.

Figure 3.2a. FAU LSX Li

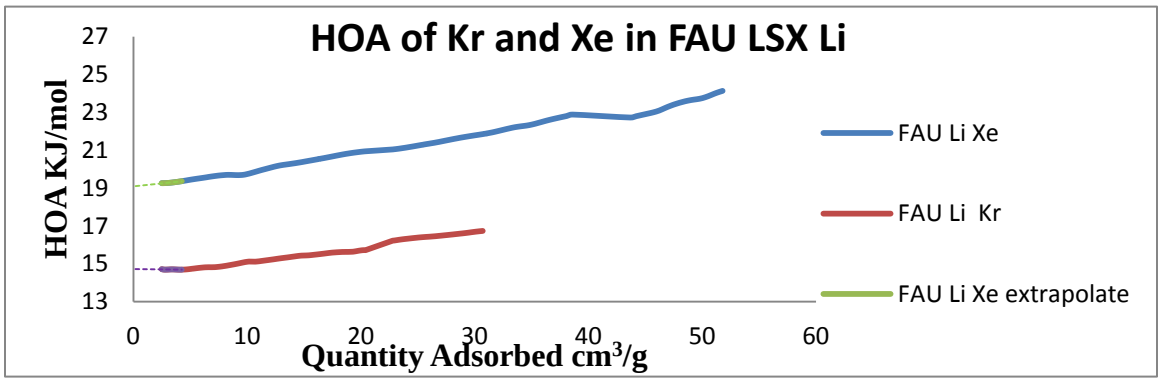

Figure 3.2b FAU LSX Na

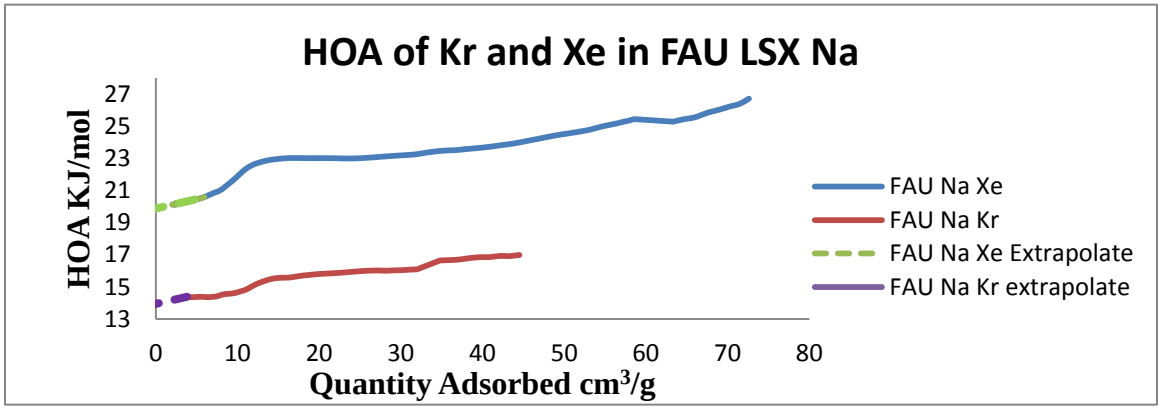

Figure 3.2c. FAU LSX K

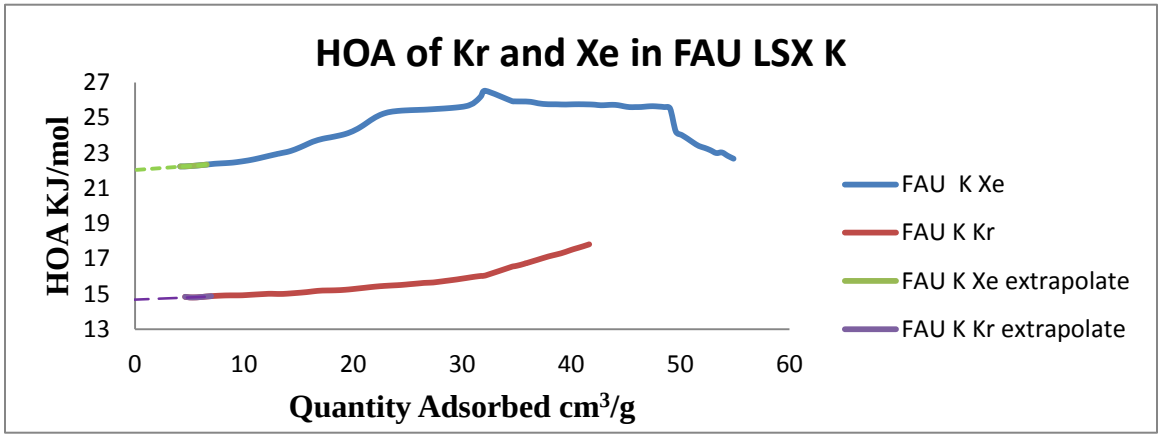

Figure 3.2. Heats of adsorption curves in Kr and Xe with different alkali metal ion-exchanged zeolite FAU LSX and extrapolations to zero coverage

Table 3.3. Extrapolated initial heats of adsorption values in Kr and Xe with different alkali metal ion-exchanged FAU LSX zeolite.

Adsorbents FAU LSX	Initial HOA kJ/mol Kr	Initial HOA kJ/mol Xe	Difference in initial HOA kJ/mol
Li	14.7	19.1	4.4
Na	13.9	19.9	6.0
K	14.6	22.0	7.4
Rb	17.5	24.7	7.2
Cs	19.0	26.0	7.0

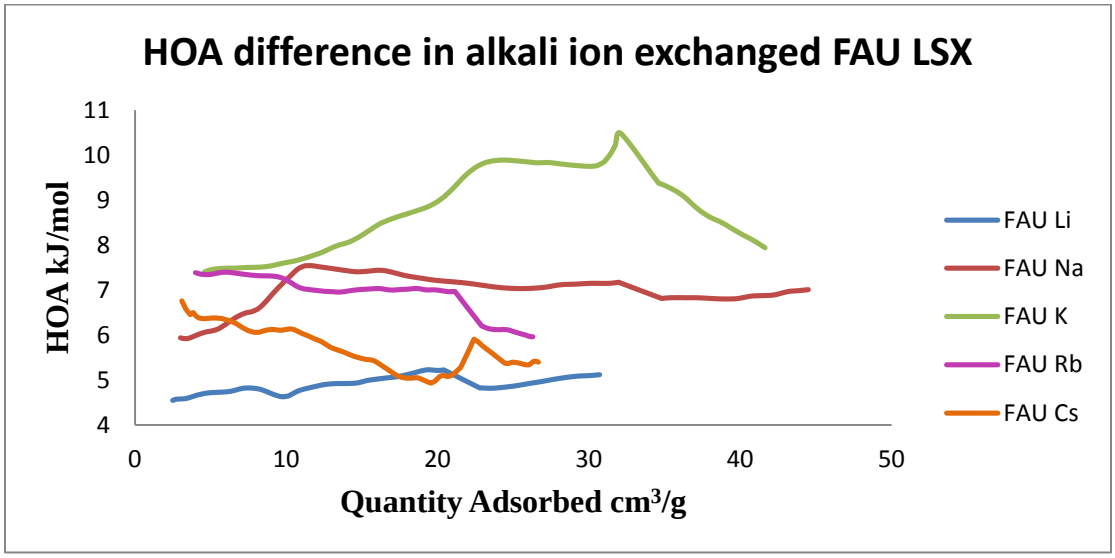

Figure 3.3. Difference in the Heats of adsorption curves in Kr and Xe with different alkali metal ion-exchanged zeolite FAU LSX.

From the figure 3.2a, 3.2b, 3.2c we can see that the values of heats of adsorption extrapolated to zero coverage for the Li, Na, K and FAU LSX with Xe are around 19.1 kJ/mol, 19.9 kJ/mol and 22.0 kJ/mol which is attributed towards adsorbate-adsorbent interaction and it increases to around 24.0 kJ/mol, 26.0 kJ/mol, 25.0 kJ/mol respectively at higher loadings. Or, this must be due to the dispersive interaction among the adsorbates. Like Xe, exactly similar trends are observed with Kr both at zero coverage and at higher loadings in all three above-mentioned zeolites. Their HOA values at higher loadings are approximately 15.0 kJ/mol. Surprisingly, the HOA of both FAU LSX Na and FAU LSX K shows an increase around 22.0 kJ/mol and 25 kJ/mol respectively at higher loadings. This could be comprehended as gas-gas interactions.

It is hard to interpret the data in Rb and Cs FAU LSX samples (Appendix II) which are ~ 34% and ~ 51% ion-exchanged. With FAU LSX, the HOA curves of both Kr and Xe remain the same. They are ~ 18 and 25 kJ/mol. This could be due to a uniform gas adsorption sites present throughout the loadings. On the other hand, FAU LSX Cs shows almost a uniform decrease in HOA with Xe with increase in loadings to 23 kJ/mol. This drop off could be accounted for the saturation of pores. However with Kr the HOA curves remain almost constant at ~ 18 kJ/mol.

From Table 3.3, we observe that the initial HOA values increase with increase in the size of cations both with Kr and Xe. For practical separations, a large difference in initial HOA suggests a better adsorbent. This shows a high selectivity of one gas over the other. We calculated the initial differences in the HOA curves between Kr and Xe in all the FAU LSX.

The increase in the order of their selectivity for Xe is LSX Li < LSX Na < LSX Cs < LSX Rb < LSX K. The experimentally-determined initial HOA difference is 4.4 < 6.0 < 7.0 < 7.2 < 7.4 kJ/mol respectively.

3.3 Gas adsorption studies in Kr and Xe with same cation but with different zeolite framework

Table 3.4. Kr and Xe atoms per supercage at 700 mm Hg in Ca ion-exchanged FAU LSX and LTA

Adsorbate	Kr			Xe		
Adsorbent	230K	240K	250K	280K	290K	300K
LTA Ca	1.13	0.89	0.73	1.07	0.97	0.86
FAU LSX Ca	3.52	2.95	2.39	4.09	3.63	3.18

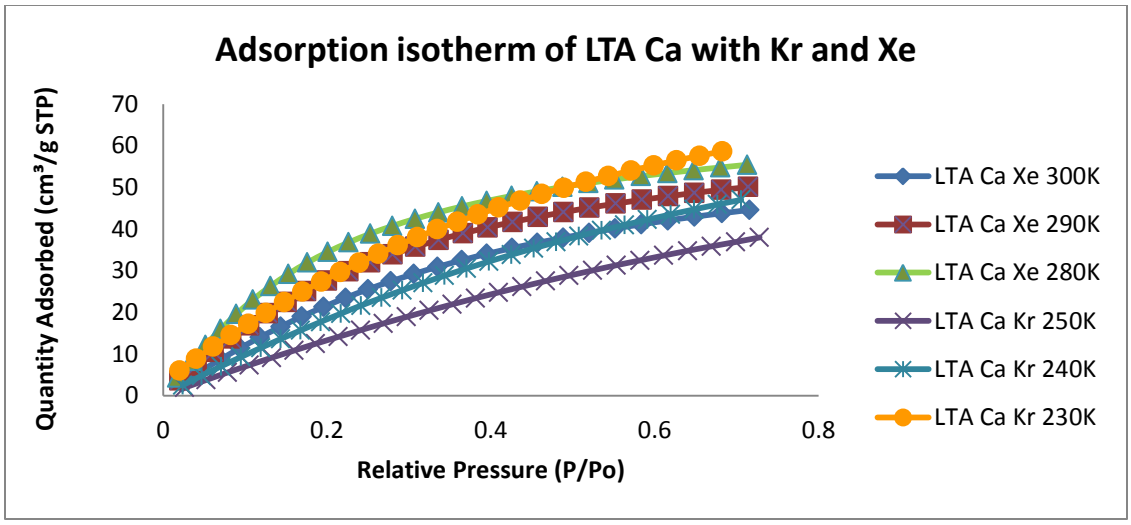

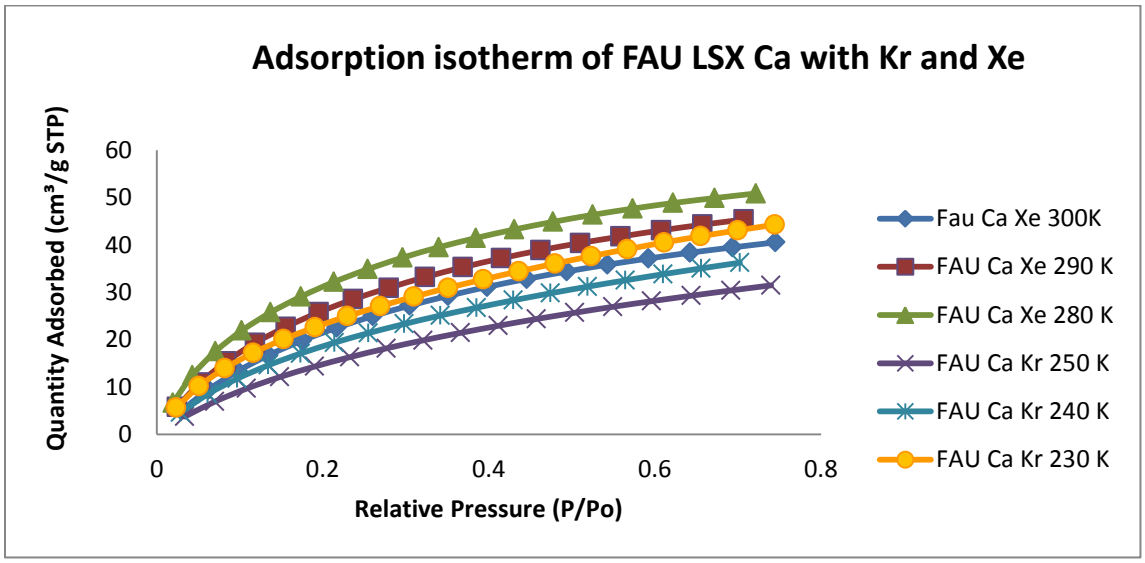

Figure 3.4.Kr and Xe adsorption isotherms in the calcium ion-exchanged zeolites with different frameworks.

From Figure 3.4, we see that among the different zeolitic frameworks with Ca^{2+} cations, both RHO Ca and GIS Ca have the smallest surface areas compared to FAU LSX Ca and LTA Ca. This suggests that the access of both Kr and Xe is hindered in RHO Ca and GIS Ca, while unrestricted in LTA Ca and FAU LSX Ca. This is very well reflected in our adsorption isotherm data (Table S5 Appendix -II). At the same time we also have to

consider that the adsorption capacities in all of the above discussed Ca ion-exchanged zeolites have not reached the asymptotic loading limit.

3.3.1. Extrapolated initial heats of adsorption in Ca ion-exchanged zeolitic frameworks

Figure 3.5a LTA Ca

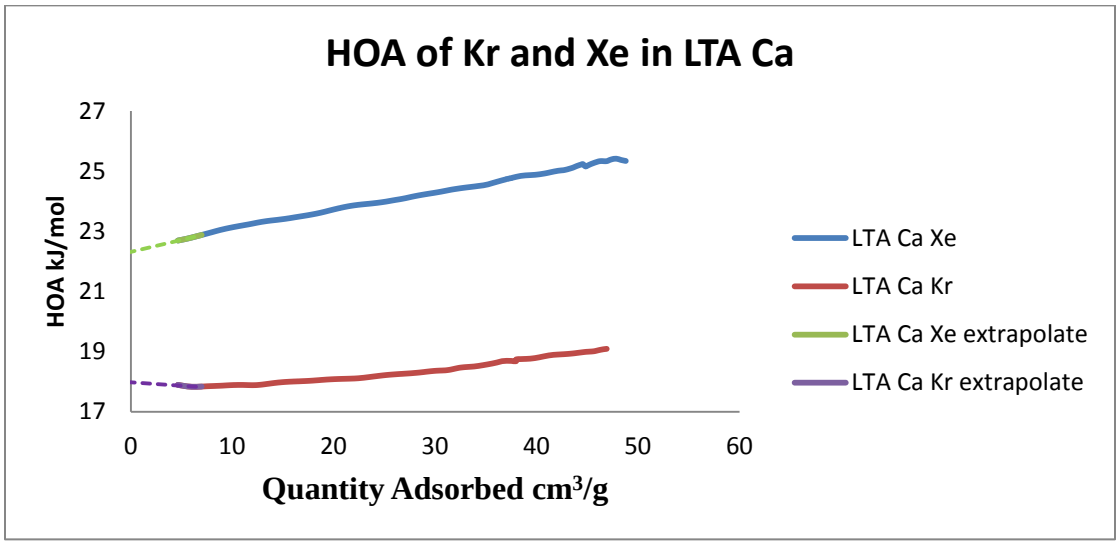

Figure 3.5b FAU LSX Ca

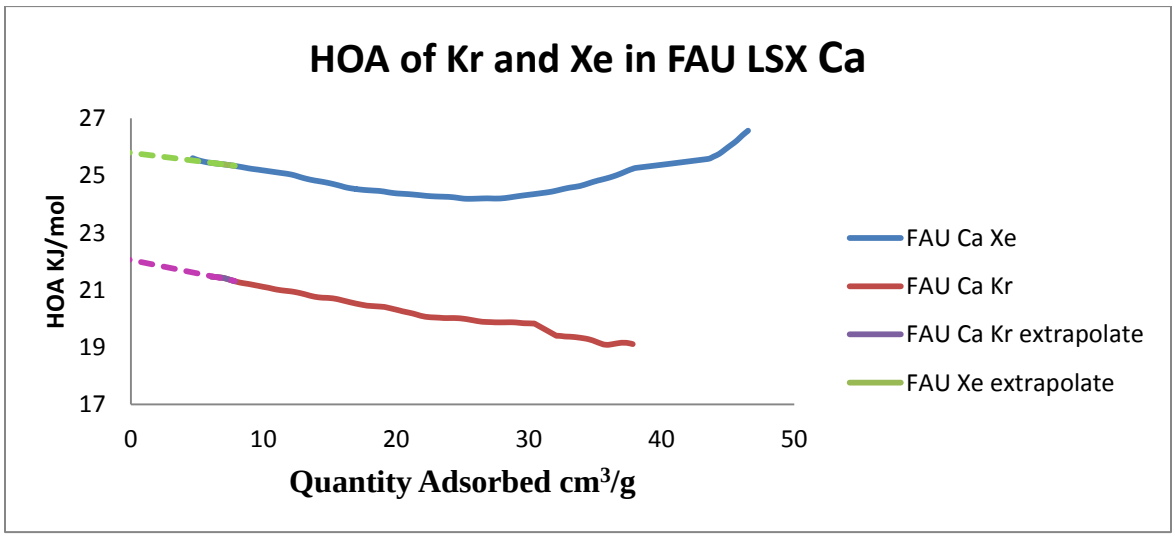

Figure 3.5. Heats of adsorption curves in Kr and Xe with calcium ion-exchanged zeolite

Table 3.5. Extrapolated Initial heats of adsorption values with Kr and Xe in calcium metal ion- exchanged LTA, FAU LSX, GIS and RHO zeolite frameworks.

Adsorbents	Initial heats of adsorption kJ/mol Kr	Initial heats of adsorption kJ/mol Xe	Difference in initial heats of adsorption kJ/mol
LTA Ca	18.0	22.3	4.3
FAU LSX Ca	22.0	25.8	3.8
RHO Ca	----------	----------	----------
GIS Ca	----------	----------	----------

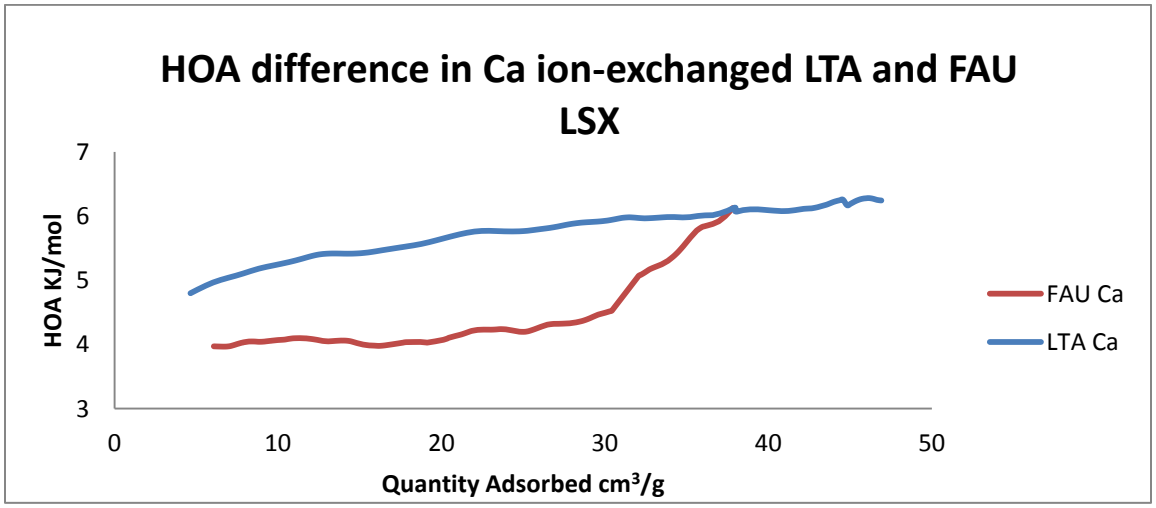

Figure 3.6. Heats of adsorption curves of Kr and Xe in calcium ion-exchanged with LTA and FAU LSX zeolitic frameworks

For LTA Ca (Figure 3.5) with Xe, HOA increases from 22.3 kJ/mol at zero coverage to around 25 kJ/mol indicating the presence of gas-gas interactions. However with Kr not much pronounced increase in HOA is observed. It remains at ~ 18 kJ/mol. With FAU LSX Ca (Figure 3.5), the HOA curve of Xe drops off initially but rises back to 26 kJ/mol at higher loadings. This is most likely due to saturation of most favorable sites. However with Kr, HOA shows a steady decrease.

As both RHO Ca and GIS Ca zeolites have comparatively smaller surface area than the other Ca zeolites, we observe a very little adsorption of Kr (Appendix II, Figure S4) at 230 K in them. We decided not to take anymore adsorption isotherm measurements and hence no heats of adsorption are measured for these zeolites**.** The difference in the initial HOA values of FAU LSX Ca and LTA Ca (Figure 3.6) are ~3.8 kJ/mol and ~ 4.3 kJ/mol.

3.4 Discussion of results

The heats of adsorption values of the zeolites in this study are calculated and their initial heats of adsorption values at zero coverage are compared in Table 3.4 and 3.5. We observe that the heats of adsorption is usually low at very low loadings and increases steadily with an increase in loadings in Li^+, Na^+ and K^+ exchanged zeolite LSX. The magnitude of increase at higher loadings is roughly around ~3-4 kJ/mol. Such increase in heats of adsorption is usually attributed to dispersion interactions between the adsorbate atoms.[4] Surprisingly, we see a hump in the heats of adsorption data at low loadings for the Na cation with both Kr and Xe. This cannot yet be completely understood. However for FAU LSX Ca we find a decrease in HOA with higher loadings. This might be accounted for the saturation of pores.[11]

The polarizability of an ion (or an atom) depends largely on the diffuseness or "how spread out" its electron cloud. For example, most positive ions have relatively small radii, and their valence electrons are held rather tightly by the excess of protons in the nucleus. Thus their polarizabilities are usually small. Hence large positive ions such as Cs^+ are significantly more polarizable than the smaller cation. Also, as the atomic number increases, the polarizability also increases. This is clearly observed in the Table 3.6.

Table 3.6. Polarizability and atomic number of cations and gases

Cations and gases	Atomic number	Polarizability α' $10^{-24}cm^3$
Li^+	2	0.029
Na^+	10	0.158
K^+	18	0.850
Rb^+	36	1.410
Cs^+	54	2.420
Ar	18	1.640
Kr	36	2.484
Xe	54	4.044

According to Talu et al[5] with FAU Y, smaller cations have higher charge density and can produce a smaller but stronger electrostatic field to polarize a CH_4 molecule. Conversely, a bigger cation creates a larger but weaker electrostatic potential. Consequently, stronger interactions are possible between smaller cations and the CH_4 molecule. For this reason, higher HOA was observed for CH_4 with smaller cations in FAU Y. Similarly, Maurin et al.[6] have argued that with FAU X, argon's HOA in the low pressure region increases with decrease in size of cation. He has explained that higher the polarization effect induced by the cations, the higher HOA. He calculated the polarization energy based on the expression[6]:

$$Ep = \frac{1}{2}\alpha E^2 = \frac{\alpha q^2 e^2}{2r^4} \qquad 3.1$$

Where "E" is the electrostatic field due to the cation and "r" corresponds to the distance between the molecule and the cation. For a given adsorbate, this polarization energy is thus proportional to q^2/r^4. This later term was evaluated for each monovalent cation (q = +1) by considering "r" as the sum of the radii of the cations $r_{M^{q+}}$ and the adsorbates (r_{Kr}, r_{Xe}).

Maurin et al.[6] have further showed a direct relationship between polarization energy of cations and the HOA with Ar. So, we expect a similar trend in our experiments with FAU LSX. But, to our surprise we observe an opposite trend. When we plot our values for the Kr and Xe initial heats of adsorption as a function of the proportional polarization energy term (Figure 3.7), we find that heats of adsorption of Kr are nearly flat, but the HOA of Xe varies inversely with polarization energy. The calculation of polarization energy and the HOA in Ar, Kr and Xe is given in Appendix II. It has to be noted that all the FAU LSX, X and Y have similar frameworks but vary in composition as follows:

FAU LSX – $Na_{96}[(AlO_2)_{96}(SiO_2)_{96}]$

FAU X – $Na_{86}[(AlO_2)_{86}(SiO_2)_{106}]$

FAU Y – $Na_{58}[(AlO_2)_{58}(SiO_2)_{134}]$

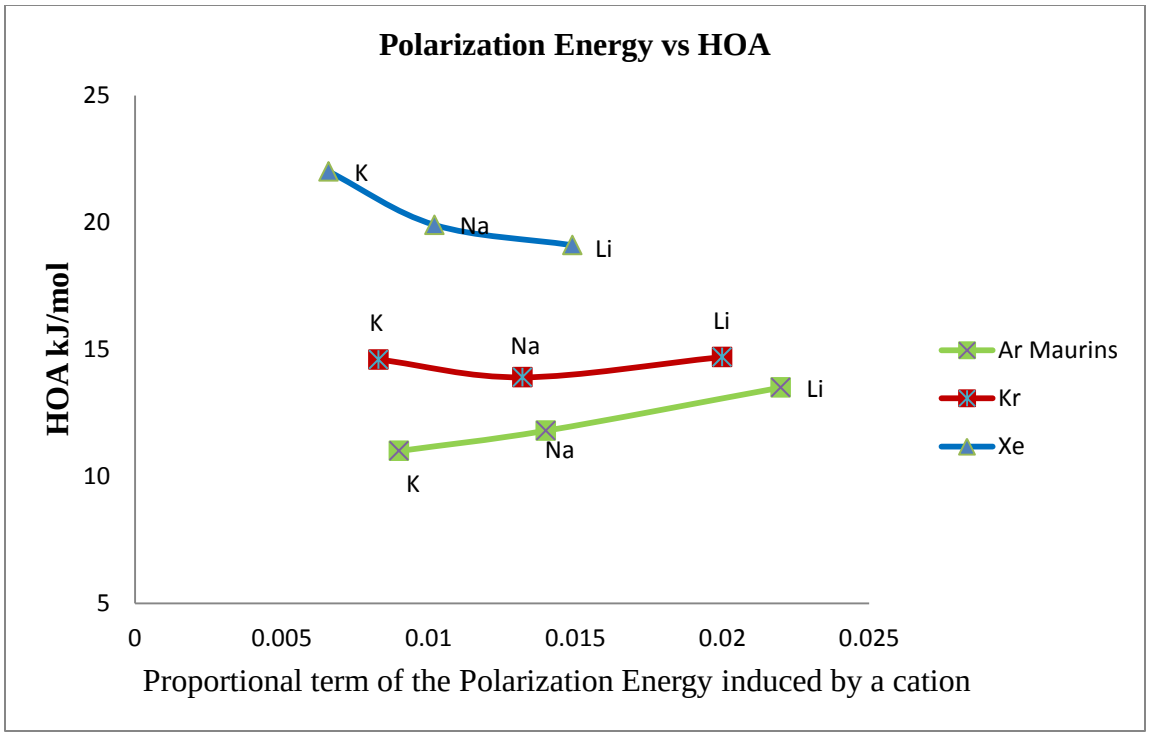

Figure 3.7. Proportional term of the polarization energy vs. HOA in Ar (Maurin), Kr and Xe with Li, Na and K cations.

Among all the other interactions contributing to the adsorption interactions, (Equation 1.3), we propose that there are two major attractive contributions to the energy of this interaction: a polarization interaction and dispersion interaction. To quantify the dispersion interactions, the London formula[7] we used provides a reasonable approximation for interactions between unlike atoms or molecules (A and B) as:

$$V = -\frac{3}{2}\frac{I_A I_B}{I_A + I_B}\frac{\alpha_A \alpha_B}{r^6}$$

Where I_A, I_B are the ionization energies of the cations and the gas. α_A, α_B are the polarizabilities of the cations and the gases and r is sum of the ionic radii of the cation

and the gas. The results of the calculations are given in Table S4 in Appendix II.

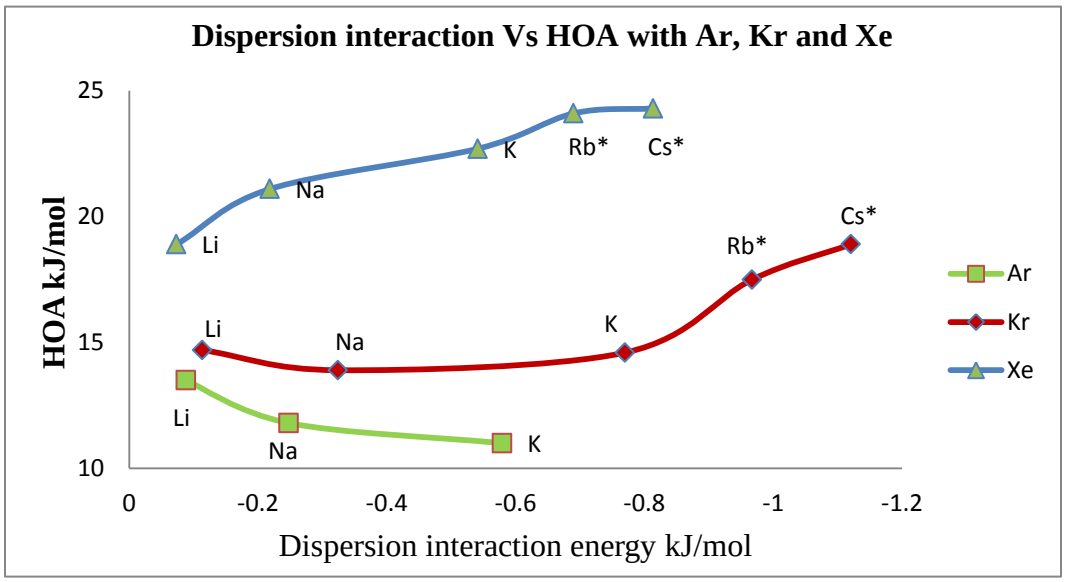

Figure 3.8. Ar, Kr and Xe dispersion interaction with the alkali cations in the zeolite frame work vs HOA

*NOTE: Rb and Cs samples are only 34% and 51% ion-exchanged.

In the case of Ar, the polarization interaction dominates. With Ar, the HOA decreases with increase in dispersion interaction. (Figure 3.8). But with Kr, the dispersion interaction becomes more important, and is slightly stronger compared to the polarization interactions. This results in virtually the same initial heats of adsorption for both low Z cations and high Z cations. However with Xe, it appears be the dispersion interaction that dominates over the other interactions. This results in higher HOA observed in FAU LSX Cs compared to FAU LSX Li with both Kr and Xe (Figure 3.8).

Moreover, we find a higher HOA of Xe than Kr in all of the ion-exchanged zeolites in our study. This can be explained due to the increased dispersive interactions in the highly polarizable Xe than Kr. So, it can be generalized that as the polarizability increases,

dispersion forces become stronger. The selectivity of one gas over the other is related by the large difference in their HOA curves.[8] Izumi et al.[9] and Jameson et al.[10] have reported that both Na A and Na X zeolites have approximate selectivity of Xe over Kr as four to six.

Soleimani et al.[11] published heats of adsorption along with temperature-programmed desorption plots for Kr and Xe in HKUST-1 (a metal organic framework). Their values at initial loading were approximately 18 and 27 kJ/mol, respectively. Recently, our group reported the gas adsorption studies of Kr and Xe by materials like Co and Ni formates. And the difference in the HOA of Xe vs Kr was found to be ~ 8 kJ/mol and ~7 kJ/mol in Co and Ni formates respectively.[12] From the present study, we recognize that FAU LSX K has the largest difference in the heats of adsorption of Xe over Kr compared to the other cations. This implies that FAU LSX K will likely have maximal selectivity among the discussed sorbents for Xe over Kr.

We also would like to consider the FAU LSX Rb and FAU LSX Cs as they have a comparable difference in the initial HOA of Kr and Xe, ~7.2 kJ/mol and ~7 kJ/mol respectively. In our experiments, both FAU LSX Rb and Cs were only partially (~ 34% and 50%) ion-exchanged. So we believe that a complete ion-exchanged FAU LSX Rb and Cs would be even more effective in the separation of Kr and Xe among the alkali ion-exchanged FAU LSX. This may also be true for FAU X, Y whose Si/Al ratio is greater than one. Alternatively, the influence of different zeolite frameworks in our gas adsorption study does not seem to be very large. As a result, we observe almost similar initial HOA difference with both FAU LSX Ca and LTA Ca as 3.8 and 4.3 kJ/mol respectively. An adsorbent with high surface area would be a good candidate for a

nonpolar and a highly polarizable adsorbate.[2] Hence, based on our study we conclude that, of the studied zeolites here, FAU LSX K would be the preferred adsorbent for Kr and Xe separation. Furthermore, if the FAU LSX Rb and Cs zeolites could be optimized towards complete ion-exchange, they would be expected to offer even higher selectivity.

3.5 Conclusion

Our aim was to find a suitable zeolitic adsorbent to separate Kr and Xe cost-effectively and environmentally friendly. The zeolitic frameworks that we studied have pore diameters comparable to that of Kr and Xe. The most remarkable feature of these zeolites is that the pores can be tailored to a wide range of sizes by ion-exchange.

We find that among the family of alkali ion-exchanged FAU LSX and the other frameworks that we have compared, FAU LSX K has the highest potential for the separation of Kr and Xe with an initial differential HOA for Xe vs Kr of ~ 7.4 kJ/mol that increases with loading. However, further exploration and development in this area is needed for a complete understanding of the adsorption process for Kr and Xe in these materials. In order to get a complete picture of interaction between the noble gases and the adsorbent, a comprehensive molecular simulation study would help to understand the observations in our study. We are also in the process of comparing the influence of different Si/Al ratios in LTA framework zeolites in the separation of Kr from Xe. This will contribute to understanding the influence of cations in the separation of Kr and Xe.

APPENDIX I

SUPPLEMENTARY INFORMATION FOR CHAPTER 2

ICP AES solution preparation

The stock solution of 1000 ppm of NaCl (VWR), KCl (Alfa Aesar), RbCl (Alfa Aesar), CsCl (Alfa Aesar), $CaCl_2$ (Alfa Aesar) and silica (sodium metasilicate) (Johnson Mathey) were prepared separately by dissolving 0.2542 g of NaCl, 0.1907 g of KCl, 0.1415 g of RbCl, 0.1267 g of CsCl and 0.2763 g of $CaCl_2$ and 0.76 g of sodium metasilicate in 100 ml of deionized water in a polypropylene volumetric flask. 2000 ppm of stock solution of Al and Li used to prepare the standards was obtained from E. Merck. A multi-element standard solution of Si, Al, Li, Na, K, Rb and Cs were prepared from their respective standard solution in the following concentrations: 5 ppm, 10 ppm, 15 ppm, 25 ppm, 40 ppm respectively. The dilution formula used for this is M1V1= M2V2.

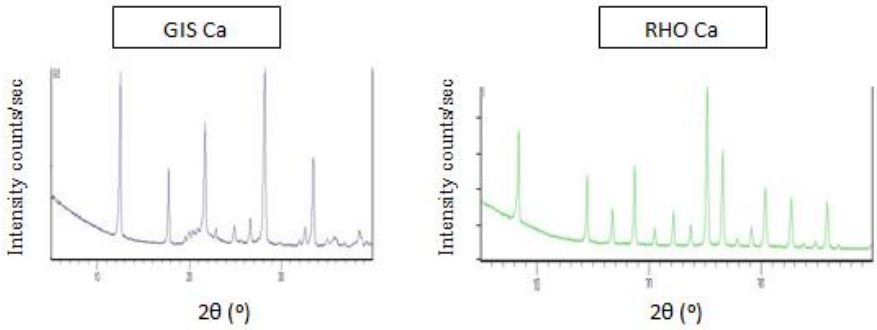

Figure S1. X-ray diffraction patterns of GIS and RHO Ca zeolites

APPENDIX II

SUPPLEMENTARY INFORMATION FOR CHAPTER 3

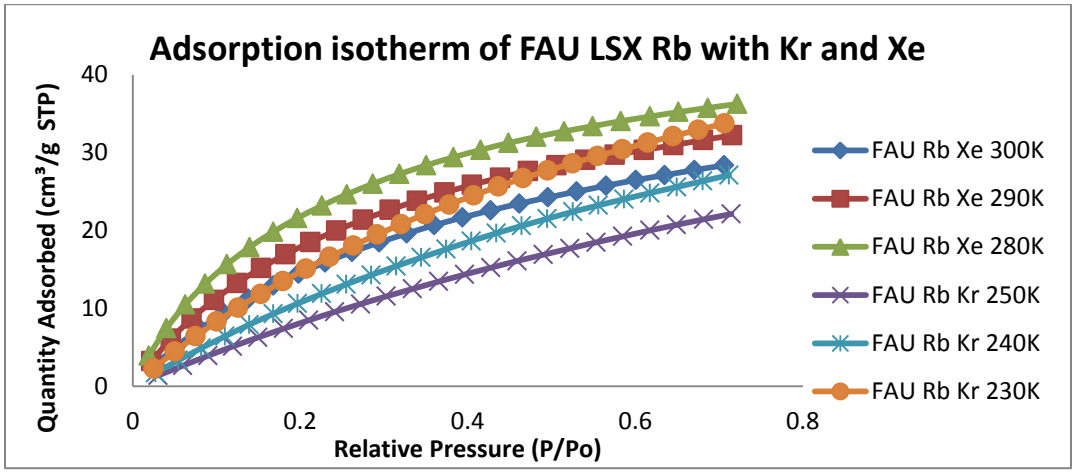

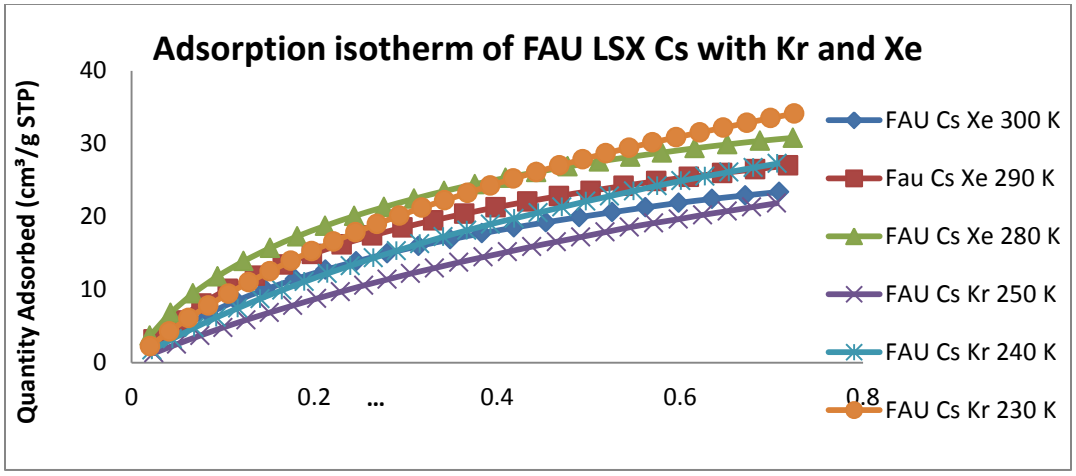

Figure S2. Kr and Xe adsorption isotherms in Rb and Cs ion-exchanged FAU LSX at different temperatures.

Table S1. Equilibrium Adsorption Capacity for Kr and Xe in alkali metal ion exchanged FAU LSX at 700 mm Hg

	Quantity adsorbed by the adsorbents in cm^3/g					
Adsorbates	Kr			Xe		
Temperature	230 K	240K	250K	280K	290K	300K
LiX NEW	43.64	30.97	21.94	63.82	52.24	40.65
NaX	60.78	44.54	33.39	82.44	72.65	60.66
KX	55.68	41.76	32.35	59.65	55.20	49.39
RbX	33.76	27.12	22.13	36.26	32.24	28.38
CsX	34.13	27.28	21.84	30.81	27.01	23.39

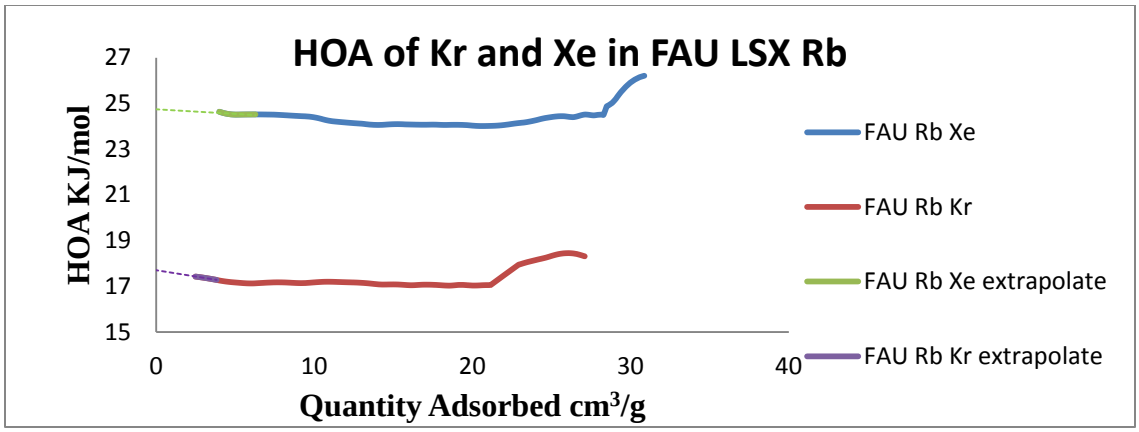

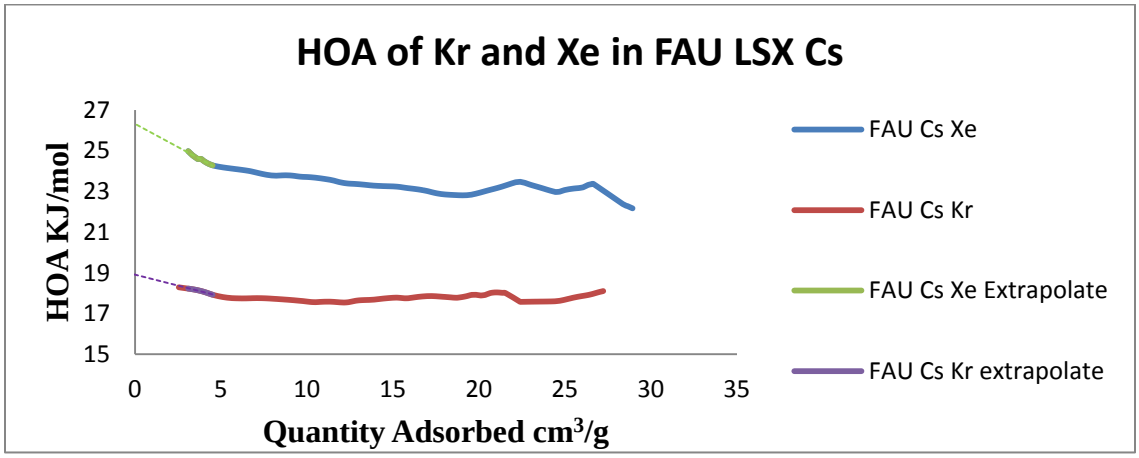

Figure S3. Heats of adsorption curves in Kr and Xe with Rb and Cs metal ion-exchanged zeolite FAU LSX and extrapolations to zero coverage

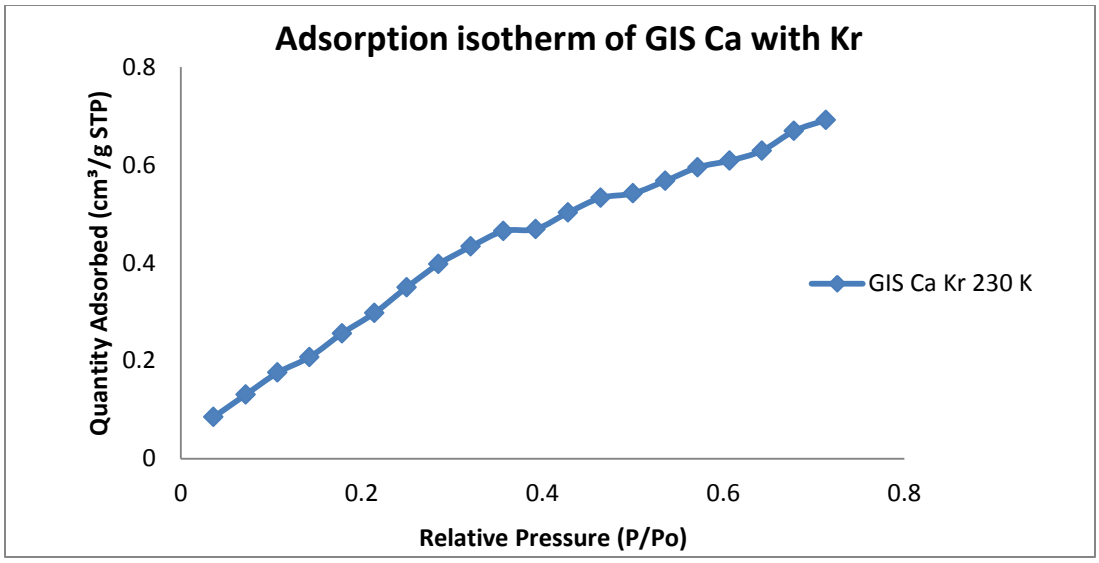

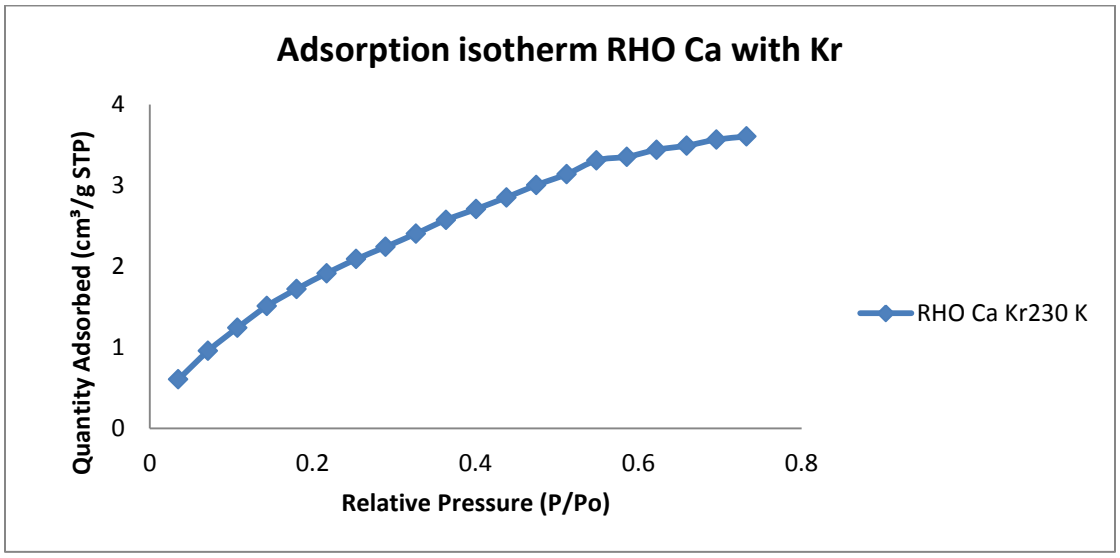

Figure S4.Kr and Xe adsorption isotherms in the calcium ion-exchanged RHO and GIS zeolites with different frameworks

Table S2. Equilibrium Adsorption Capacity for Kr and Xe in calcium metal ion exchanged LTA, FAU LSX, GIS, and RHO at 700 mm of Hg.

	Quantity adsorbed by the adsorbents in cm^3/g					
Adsorbates	Kr			Xe		
Temperature	230 K	240K	250K	280K	290K	300K
Ca LTA	58.69	45.91	37.99	55.44	50.09	44.59
Ca FAU LSX	45.36	38.02	30.88	52.74	46.94	41.05
RHO Ca	3.605	---------	---------	---------	---------	---------
GIS Ca	0.692	---------	---------	---------	---------	---------

Table S3.

The proportional term for the polarization energy (PE) induced by an isolated cation is:

PE term = $\frac{q2}{(\text{radsorbate}+r_{M\,q+})4}$. Using this formula we calculated the proportional term for the polarization energy induced by the cation in Kr and Xe. This was compared against the HOA kJ/mol calculated from our experimental data.

With Ar 1.92 Å**

Cation	Radii *	HOA KJ/mol	PE term
Lithium	0.68	13.5	0.022
Sodium	0.97	11.8	0.014
Potassium	1.33	11	0.009

With Kr 1.98 Å**

Cation	Radii *	HOA KJ/mol	PE term
Lithium	0.68	14.7	0.02
Sodium	0.97	13.9	0.0132
Potassium	1.33	14.6	0.0083

With Xe 2.18 Å **

Cation	Radii *	HOA KJ/mol	PE term
Lithium	0.68	19.1	0.0149
Sodium	0.97	19.9	0.0102
Potassium	1.33	22	0.0066

Table S4.

We calculated the dispersion interaction by using the London formula with Ar (Maurin), Kr and Xe:

$$V = -\frac{3}{2}\frac{I_A I_B}{I_A + I_B}\frac{\alpha_A \alpha_B}{r^6}$$

Cation	Sum of ionic radii of cation and Ar (r) Å	Polarizability α' 10^{-24}cm^3	Ionization Energy I_A kJ/mol ***	Dispersion interaction kJ/mol	HOA kJ/mol
Li	2.6	0.029	513.3	-0.088	13.5
Na	2.89	0.158	495.8	-0.248	11.8
K	3.25	0.85	418.8	-0.579	11.0
Ar		1.63	1520.4		

Cation	Sum of ionic radii of cation and Kr (r) Å	Polarizability α' 10^{-24}cm^3	Ionization Energy I_A kJ/mol ***	Dispersion interaction kJ/mol	HOA kJ/mol
Li	2.66	0.029	513.3	-0.113	14.7
Na	2.95	0.158	495.8	-0.324	13.9
K	3.31	0.85	418.8	-0.770	14.6
Rb	3.45	1.41	403.0	-0.967	17.5
Cs	3.65	2.42	375.5	-1.121	18.9
Kr		2.48	1350.7		

Cation	Sum of ionic radii of cation and Xe (r)Å	Polarizability α' 10^{-24}cm^3	Ionization Energy I_A kJ/mol ***	Dispersion interaction kJ/mol	HOA kJ/mol
Li	2.86	0.029	513.3	-0.073	18.9
Na	3.15	0.158	495.8	-0.219	21.1
K	3.51	0.850	418.8	-0.542	22.7
Rb	3.65	1.410	403.0	-0.690	24.1
Cs	3.85	2.420	375.5	-0.814	24.3
Xe		4.04	1170.4		

* Ionic Radii of cations - Walton, K. S.,Abney, M. B.,Douglas LeVan, M. Microporous Mesoporous Mater. 91, 78–84, **2006.**

** Atomic radius of gases used - Zhang , Xu American Mineralogist, 80, 670-675, **1995**.

*** Ionization energy - Physical Chemistry by Peter Atkins and Julio de Paula, Mar 10, **2006.**

Polarizability

Yang, R. T., Adsorbents Fundamentals and Applications, John Wiley & Sons, Hoboken,

2003.

Barrer, R. M., Stuart, W. I., Proceedings of the Royal Society of London, Series A,

Mathematical and Physical Sciences, 249, 1259, 464-483, **1959.**

Table S5.

Adsorbents and the corresponding surface area

Adsorbent	BET surface area (m^2/ g)	Pore volume (cm^3/ g)
LTA Ca	620	0.237
RHO Ca	21	0.007
GIS Ca	11	0.004
Ca LSX	567	0.217
LI LSX	778	0.299
Na LSX	890	0.343
K LSX	611	0.236
Rb LSX	404	0.156
Cs LSX	418	0.159

Table S6.

Quantity adsorbed, HOA and uncertainty of Kr and Xe in FAU LSX K

Xe			Kr		
Quantity Adsorbed cm^3/g	HOA kJ/mol	Uncertainty kJ/mol	Quantity Adsorbed cm^3/g	HOA kJ/mol	Uncertainty kJ/mol
3	22.394	0	1.7	14.201	0
3.5293	22.41	0	2.1061	14.824	0.312
4.0586	22.235	0.119	2.5121	14.86	0.3
4.5879	22.237	0.146	2.9182	14.885	0.278
5.1172	22.258	0.162	3.3242	14.905	0.246
5.6465	22.284	0.159	3.7303	14.911	0.199
6.1758	22.314	0.143	4.1364	14.887	0.169
6.7051	22.347	0.135	4.5424	14.84	0.166
7.2343	22.382	0.134	4.9485	14.806	0.179
7.7636	22.404	0.136	5.3545	14.8	0.192
8.2929	22.421	0.14	5.7606	14.809	0.204
8.8222	22.444	0.145	6.1667	14.829	0.213
9.3515	22.481	0.158	6.5727	14.853	0.214
9.8808	22.527	0.172	6.9788	14.873	0.212
10.4101	22.579	0.183	7.3848	14.888	0.209
10.9394	22.642	0.189	7.7909	14.901	0.206
11.4687	22.715	0.192	8.197	14.91	0.2
11.998	22.793	0.19	8.603	14.915	0.194
12.5273	22.87	0.184	9.0091	14.916	0.188
13.0566	22.943	0.175	9.4152	14.917	0.182
13.5859	23.012	0.166	9.8212	14.921	0.169
14.1152	23.085	0.154	10.2273	14.936	0.151
14.6444	23.194	0.134	10.6333	14.951	0.133
15.1737	23.327	0.136	11.0394	14.966	0.116
15.703	23.474	0.151	11.4455	14.98	0.1
16.2323	23.62	0.168	11.8515	14.994	0.086
16.7616	23.732	0.165	12.2576	15.007	0.075
17.2909	23.814	0.144	12.6636	15.005	0.074
17.8202	23.874	0.153	13.0697	14.997	0.078
18.3495	23.939	0.189	13.4758	14.998	0.078
18.8788	24.01	0.209	13.8818	15.011	0.074
19.4081	24.101	0.196	14.2879	15.029	0.074
19.9374	24.227	0.148	14.6939	15.048	0.077
20.4667	24.393	0.071	15.1	15.067	0.084
20.996	24.598	0.016	15.5061	15.089	0.091

21.5253	24.825	0.019	15.9121	15.115	0.097
22.0545	25.029	0.045	16.3182	15.145	0.099
22.5838	25.185	0.069	16.7242	15.172	0.102
23.1131	25.292	0.099	17.1303	15.189	0.11
23.6424	25.353	0.138	17.5364	15.195	0.12
24.1717	25.388	0.166	17.9424	15.199	0.13
24.701	25.411	0.143	18.3485	15.204	0.144
25.2303	25.426	0.091	18.7545	15.214	0.159
25.7596	25.438	0.024	19.1606	15.229	0.164
26.2889	25.449	0.048	19.5667	15.25	0.157
26.8182	25.464	0.118	19.9727	15.275	0.144
27.3475	25.485	0.173	20.3788	15.302	0.13
27.8768	25.505	0.198	20.7848	15.329	0.117
28.4061	25.526	0.184	21.1909	15.358	0.106
28.9354	25.55	0.162	21.597	15.386	0.097
29.4646	25.579	0.131	22.003	15.411	0.092
29.9939	25.618	0.084	22.4091	15.434	0.085
30.5232	25.679	0.018	22.8152	15.452	0.074
31.0525	25.836	0.048	23.2212	15.467	0.062
31.5818	26.125	0.125	23.6273	15.481	0.05
32.1111	26.527	0.204	24.0333	15.494	0.037
32.6404	26.811	0.231	24.4394	15.51	0.023
33.1697	26.745	0.168	24.8455	15.532	0.006
33.699	26.186	0.103	25.2515	15.555	0.001
34.2283	25.948	0.189	25.6576	15.577	0.002
34.7576	25.928	0.188	26.0636	15.599	0.008
35.2869	25.921	0.179	26.4697	15.623	0.021
35.8162	25.92	0.156	26.8758	15.634	0.046
36.3455	25.893	0.122	27.2818	15.646	0.069
36.8747	25.828	0.125	27.6879	15.675	0.067
37.404	25.781	0.133	28.0939	15.707	0.052
37.9333	25.763	0.131	28.5	15.74	0.043
38.4626	25.761	0.132	28.9061	15.772	0.057
38.9919	25.753	0.144	29.3121	15.805	0.091
39.5212	25.748	0.159	29.7182	15.841	0.125
40.0505	25.758	0.187	30.1242	15.879	0.139
40.5798	25.763	0.223	30.5303	15.917	0.147
41.1091	25.761	0.26	30.9364	15.957	0.153
41.6384	25.753	0.285	31.3424	15.992	0.157
42.1677	25.737	0.3	31.7485	16.02	0.161
42.697	25.705	0.31	32.1545	16.046	0.164
43.2263	25.718	0.365			
43.7556	25.733	0.418			

44.2848	25.711	0.446			
44.8141	25.646	0.459			
45.3434	25.599	0.463			
45.8727	25.603	0.491			
46.402	25.607	0.518			
46.9313	25.638	0.561			
47.4606	25.652	0.59			
47.9899	25.633	0.616			
48.5192	25.602	0.652			
49.0485	25.523	0.692			

This is a representation of what we see in error bars in all the other analyzed zeolites in this study. Estimation of errors is solely from linear regression and other experimental errors are not included.

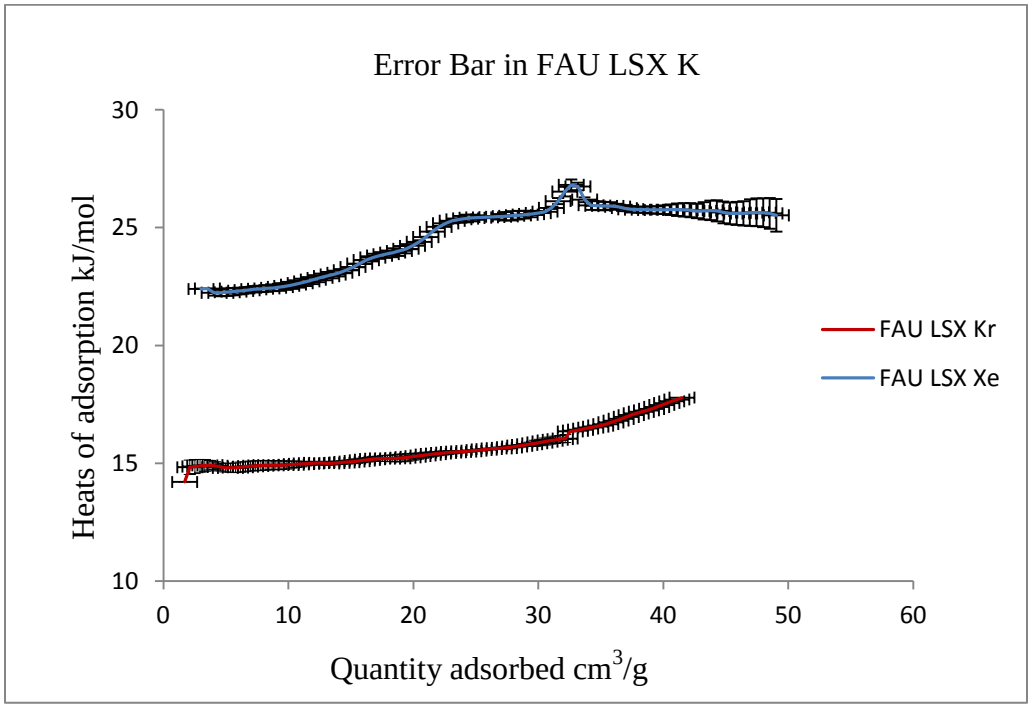

REFERENCES

CHAPTER 1 (1-67)

1. Yang, R. T., Adsorbents: Fundamental and Applications, John Wiley, Hoboken, NJ, **2003**.

2. Izumi, J., Auerbach, S. M., Carrado, K. A., Dutta, P. K., Eds, In Handbook of Zeolite Science and Technology, CRC Press, New York, **2003**.

3. Elvers, B., Hawkins, S., Ullmann's Encyclopedia of Industrial Chemistry, Weinheim, VCH Verlaggesellschaft GmbH, Vol. A 28, 475-504, **1996**.

4. Jacobs, P. A., Martens, J. A., Synthesis of High-Silica Aluminosilicate Zeolites, Amsterdam, Elsevier, **1987**.

5. Rouqerol, J., Avnir, D., Fairbridge, C. W., Everett, D. H., Haynes, J.H., Pernicone, N., Ramsay, J. D., Sing, K. S. W., Unger, K.K., Pure Appl. Chem. 66, 1739, **1994**.

6. Breck, D. W., Zeolite Molecular Sieves: Structure, Chemistry and Use, Wiley and Sons, London, **1974**.

7. Qinhua, Xn., Aizhen, Yan., Hydrothermal Synthesis and Crystallization of Zeolites. in: Hydrothermal Growth of Crystals, K. Byrappa, ed., Prog. Crystal Growth and Characterization, 21:29–70, **1990**.

8. Lowenstein, W., American Mineralogist 39, 92-96, **1954**.

9. Proctor & Gamble, http://www.scienceinthebox.com/en_UK/glossary/buildersen.html.

10. Dessau, R. M., Schlenker, J. L., Higgins, J. B. *Zeolites* 10, 522, **1990**.

11. Chen, N. Y., Degnan, T. F., Jr. Smith., C. M., *Molecular Transport and Reaction in Zeolites*, VCH, New York, **1994**.

12. Eastermann, M., McCusker, L. B., Barchaloer, Ch., Merrouche, A., Kessler, H., Nature, 320, **1991**.

13. Barchaloer, C., Meier, W. H., Olson, D. H., Atlas of zeolite framework types, 6th Edition, Elsevier, 2007. http://www.iza-structure.org/databases/

14. Yang, R. T., Activated Carbon, in Adsorbents, Fundamentals and Applications, John Wiley & Sons, Inc., Hoboken, NJ, **2003**.

15. Breck, D. W., Zeolite Molecular Sieves, Wiley, **1974**.

16. Argauer, R. J., Landolt, G. R., U.S. Patent 3, 702, 886, **1972**.

17. Barrer, R.M., J. Chem. Soc. Faraday Trans. 86, 1123–1130, **1990**.

18. Bakker, W.J.W., van den Broeke, L.J.P., Kapteijn, F., Moulijn, J.A. AIChEJ, 43, 2203–2214, **1997**.

19. Yang, R. T., Gas separation by adsorption processes, 1st ed., 7-25, Butterworth, Boston, USA, **1987**.

20. Chao, C. C., U.S. Patent 4,859, 217, **1989**.

21. Neuzil, R.W. U.S. Patent 3558730; U.S. patent 3558732; U.S. patent 3626020 **1971**.

22. Kulprathipanja, S., U.S. Patent 1995 and U.S.Patent, **1999**.

23. Hotlier, G., Balannec, B., From batch elution to simulated counter current chromatography, Oil and Gas Science and Technology, 46, 803, **1991**.

24. Gas adsorption group, Retrieved August 21,2013, from http://chemelab.ucsd.edu/aeronex02/background.html

25. Marcilly, C., Present status and future trends in catalysis and refining in petro chemicals. J. Catal. 216, 47-62, **2003**.

26. Hagen A., Roessner F., Conversion of Ethane into Aromatic Hydrocarbons on Zinc Containing ZSM-5 Zeolites Prepared by Solid State Ion Exchange Studies in Surface Science and Catalysis, 83 (C), 313-320, **1994**.

27. Csicsery, S., M. Shape-Selective Catalysis in Zeolites, 4, 202-213, **1984**.

28. Townsend, R. P., Coker E. N., Ion exchange in zeolites, Stud. Surf. Sci. Catal, 137,467, **2001**.

29. Vaughan, D. E. W., Chem. Eng. Prog. Feb., 25, **1988**.

30. Bell, R.G., May 2001, Retrieved August 21,2013, from www.bza.org/zeolites.html

31. Breck, D., Zeolite Molecular Sieves: Structure, Chemistry and Use, Krieger Pub. Co, Malabar, FL, **1984**.

32. Jeffroy, M., Boutin, A., Fuchs, A. H., Understanding the Equilibrium Ion Exchange Properties in Faujasite Zeolite from Monte Carlo Simulations, J. Phys. Chem. B, 115, 15059−15066, **2011**.

33. Dyer, A., An Introduction to Zeolite Molecular Sieves, John Wiley & Sons, **1988**.

34. McCusker, L. B., Liebau, F., Engelhardt, G., Pure Appl Chem, 73, 381, **2001**.

35. Baerlocher, C., McCusker, L. B., Database of Zeolite Structures: http://www.iza-structure.org/databases/ **2013**.

36. Corma, A., Zeolites in Oil Refining and Petrochemistry, Zeolite Microporous Solids, Synthesis, Structure, and Reactivity, Kluwer Academic, The Netherlands, **1992**.

37. Sherry, H.S., Marinsky, J.A., ed. Advances in Ion Exchange, Vol 2. New York: Marcel Dekker, 89–133, **1969**.

38. Walton, K. S., Abney, M. B., Douglas Le Van, M. Microporous Mesoporous Mater, 91, 78–84, **2006**.

39. Salla, I., Salagre, P., Cesteros, Y., Medina, F., Sueiras, J.E., J. Phys. Chem. B, 108, 5359, **2004.**

40. Macedonia, M.D., Moore, D.D., Maginn, E.J., Olken, Langmuir, 16, 3823, **2000**.

41. Savitz, S., Myers, A.L., Gorte, R.J., Microporous. Mesoporous. Mater, 37, 33, **2000**.

42. Corma, A., J. Catal. 2161 (2), 298, **2003**.

43. Bezus, A.G., Kiselev, A.V., Sedlacek, Z., Du. Pham Quang, J. Chem. Soc. Faraday Trans I, 67, 468, **1971**.

44. Barrer, R.M., Gibbons R.M., Soc., J. Chem. Faraday Trans. I, 61, 948, **1965**.

45. Dzhigit, O.M., Kiselev, A.V., Mikos, K.N., Muttik, G.G., Rahmanova, T.A., J. Chem. Soc. Faraday Trans. I, 67, 458, **1971**.

46. Yang, S., Navrotsky, A., Micropor. Mesopor. Mater. 37, 175, **2000**.

47. Auerbach, S. M., Carrado K. A., Dutta, P. K., Handbook of Zeolite Science and Technology, Marcel Dekker, Inc., New York, **2003**.

48. Duong, D. D., Adsorption Analysis: Equilibria and Kinetics, Imperial College Press, London, **1998**.

49. Seader, J., Henley, J., Separation Process Principles, Wiley, New York, **1998**.

50. Chackett, K.F., Tuck, D.G., Trans. Faraday Soc. 53, 1652, **1957**.

51. Jameson, C.J., Jameson, A.K., H.M. Lim, J. Chem. Phys. 107, 4364, **1997**.

52. Hutson, N.D., Yang, R.T., AIChE J. 46, 2305, **2000**.

53. Maurin, G., Llewellyn, P. L., Poyet, T. H., Kuchta, B., Microporous Mesoporous Mater. 79, 53–59, **2005**.

54. Ryan, P., Farha, O. K., Broadbelt, L. J., Snurr, R. Q. AIChEJ. 57, 1759-1766, **2011**.

55. Böhlmann, W., Pöppl, A., Sabo, M., Kaskel, S., J. Phys. Chem. B, 110, 20177-20181, **2006**.

56. King, C. J., Separation Progress, McGraw-Hill, New York, 2nd edn, **1980**.

57. Karger, B. L., Snyder R. L., Horvath, H., An Introduction to Separation Science, Wiley, New York, **1973**.

58. Yang, R. T., Adsorbents Fundamentals and Applications, John Wiley & Sons, Hoboken, **2003**.

59. Yang, R.T., Gas Separation by Adsorption Progress, Butterworth, Boston, **1987**.

60. Li, R., Kuppler, R.J., Zhou H.C., Selective gas adsorption and separation in metal-organic frameworks, Chem. Soc. Rev., 38, 1477–1504, **2009**.

61 Lide, D. R., CRC Handbook of Chemistry and Physics, CRC Press, 88th edn, **2007**.

62 Sircar, S., Ind. Eng. Chem. Res., 45, 5435–5448, **2006**.

63 Rouquerol, F., Rouquerol, J., Sing, K., Adsorption by Powder & Porous Solid, Academic Press, London, **1999**.

64 Breck, W., Zeolites Molecular Sieves: Structure, Chemistry and Use; Wiley-InterScience: New York, **1974**.

65 Barrer, R. M., Zeolites and Clay Minerals. Academic Press, New York, **1978**.

66 Karacan, Ö.C., Okandan E., Assessment of energetic heterogeneity of coals for gas adsorption and its effect on mixture predictions for coal bed methane studies**,** Fuel, 79, 1963-1974, **2000**.

67 Sakuth, M., Meyer J., Gmehling J., Measurement and prediction of binary adsorption equilibria of vapors on dealuminated Y-zeolites (DAY), Chemical Engineering and Processing, 37, 267-277, **1998**.

CHAPTER 2 (1- 7)

1. Robson, H., Verified Syntheses of Zeolitic Materials. Amsterdam, Elsevier, **2001**.

2. Ackley, M.W., Yang, R.T., Diffusion in ion-exchanged clinoptilolites, AIChE J. 37: 1645–1656, **1991**.

3. www.scn.org/~bh162/making_molar_&_normal_solutions.

4. Kevin, R., Franklin, D., Townsend, P., J. Chem. SOC., Faraday Trans I, 81, 1071-1086, **1985**.

5. Chao, K. J., Chen, S. H., Yang M. H., Fresenius Z Anal Chem. 331:418-422, **1988**.

6. Certain trade names and company products are mentioned in this paper to adequately specify the experimental procedure and equipment used. In no case does this imply recommendation or endorsement by NIST, nor does it imply that the products are necessarily the best available for this purpose.

7. Walton, K. S., Snurr, R. Q. J. Am. Chem. Soc. 129, 8552-8556, **2007**.

CHAPTER 3 (1-12)

1. Rege, S. U., Yang, R. T., Buzanowski, M. A. Sorbents for air pre purification in air separation. Chem. Eng. Sci. 55, 4827–4838, **2000**.

2. Li, R., Kuppler, R.J., Zhou H.C., Selective gas adsorption and separation in metal-organic frameworks, Chem. Soc. Rev. 38, 1477–1504, **2009**.

3. Sircar, S., Ind. Eng. Chem. Res. 45, 5435–5448, **2006**.

4. Barrer, R.M., Zeolites and Clay Minerals as Sorbents and Molecular Sieves, Academic press, **1978**.

5. Talu, O., Zhang, S.Y., Hayhurst, D. T., J. Phys. Chem. 97, 12894–12898, **1993**.

6. Maurin, G., Bell, R., Kuchta, B., Poyet, T., Llewellyn, P. Adsorption, 11, 331–336, **2005**.

7. Physical Chemistry by Peter Atkins and Julio de Paula, Mar 10, **2006**.
8. Ryan, P., Farha, O. K., Broadbelt L. J., Snurr, R. Q., AIChE J., 57,1759–1766, **2011**.

9. Izumi, J. In Handbook of Zeolite Science and Technology; Auerbach, S. M., Carrado, K. A., Dutta, P. K., Eds. CRC Press: New York, **2003**.

10. Jameson, C.J., Jameson, A.K., Lim, H.M., J. Chem. Phys. 107, 4364, **1997**.

11. Soleimani Dorcheh, A., Dinnebier, R. E., Kuc, A., Magdysyuk, O., Adams, F., Denysenko, D., Heine, T., Volkmer, D., Donner, W., Hirscher, M. Phys. Chem. Chem. Phys. 14, 12892-12897, **2012**.

12. Lawler, K.V., Hulvey, Z., Forster, P.M., Chem. Commun., 49 (93), 10959 – 10961, **2013**.

VITA

Graduate College
University of Nevada, Las Vegas

Breetha Alagappan

Degrees:

Bachelor of Science in Chemistry, Manonmaniam Sundaranar University, 2000

Tirunelveli, India.

Master of Science in Chemistry, Madras University, 2002

Chennai, India.

Special Honors and Awards:

1999-2000 Most Outstanding Undergraduate in Chemistry Department: Manonmaniam Sundaranar University, 2000, Tirunelveli, India.

2003-National Award for the best essay in "Petroleum Conservation and Green house Gas emissions" Indian Oil Corporation Ltd.

Paper: "Assessing different Zeolitic adsorbents for their potential use in Kr and Xe separation" in process.

Thesis Title:

Assessing different Zeolitic adsorbents for their potential use in Kr and Xe separation

Dissertation Examination Committee:

Chairperson, Dr. Paul Forster, Ph. D.

Committee Member, Dr. Clemens Heske, Ph. D.

Committee Member, Dr. Balakrishnan Naduvalath, Ph. D.

Graduate College Representative, Dr. Venkatesan Muthukumar, Ph. D.

[7]